



**Dallas-Fort Worth Modeling Support:
Improving the Representation of
Vertical Mixing Processes in CAMx
Final Report
WO 582-11-10365-FY11-02**

Prepared for:
Doug Boyer
TCEQ
12100 Park 35 Circle
Austin, TX 78753

Prepared by:
ENVIRON International Corporation
773 San Marin Drive, Suite 2115
Novato, California, 94945
www.vironcorp.com
P-415-899-0700
F-415-899-0707

August 2011
Project Number:
06-26408B

Contents

	Page
EXECUTIVE SUMMARY	1
1.0 INTRODUCTION	2
1.1 Approach	2
2.0 REVIEW OF TWO PBL SCHEMES IN WRF	4
2.1. YSU PBL Scheme	4
2.2. MYJ PBL Scheme	5
2.3 KVPATCH	6
3. CAMX MODELING	7
3.1. CAMx Inputs	7
3.2. CAMx Results Using WRF With YSU PBL	8
3.3. CAMx Results Using WRF With MYJ PBL	18
4.0 FINDINGS AND DISCUSSION	31
4.0 REFERENCES	34
 APPENDICES	
Appendix A: Time Series of Layer 1 vertical diffusivities, ozone, and NO _x Using Meteorology from WRF with the YSU PBL scheme	
Appendix B: Time Series of Layer 1 vertical diffusivities, ozone, and NO _x Using Meteorology from WRF with the MYJ PBL scheme	
 TABLES	
Table 3-1. Comparison of 8 AM layer 1 vertical diffusivities, ozone and NO _x at Hinton when using WRF/YSU meteorology.	12
Table 3-2. Comparison of 2 PM layer 1 vertical diffusivities, ozone and NO _x at Hinton when using WRF/YSU meteorology.	15
Table 3-3. Comparison of 7 PM layer 1 vertical diffusivities, ozone and NO _x at Hinton when using WRF/YSU meteorology.	18
Table 3-4. Comparison of 8 AM layer 1 vertical diffusivities, ozone and NO _x at Hinton when using WRF/MYJ meteorology.	24
Table 3-5. Comparison of 2 PM layer 1 vertical diffusivities, ozone and NO _x at Hinton when using WRF/MYJ meteorology.	28
Table 3-6. Comparison of 7 PM layer 1 vertical diffusivities, ozone and NO _x at Hinton when using WRF/MYJ meteorology.	28

FIGURES

Figure 3-1.	Spatial plots of daily maximum 1-hour ozone on June 9 when using WRF/YSU meteorology with different vertical diffusivity inputs (top row, bottom left), and using TCEQ base case inputs (bottom right).	9
Figure 3-2.	Time series of hourly Kv's (top), ozone (middle), and NOx (bottom) from CAMx layer 1 at Denton when using OB70, YSU, and CMAQ Kv's from WRF/YSU.	10
Figure 3-3.	Time series of hourly Kv's (top), ozone (middle), and NOx (bottom) from CAMx layer 1 at Grapevine when using OB70, YSU, and CMAQ Kv's from WRF/YSU.	11
Figure 3-4.	Time series of hourly Kv's (top), ozone (middle), and NOx (bottom) from CAMx layer 1 at Hinton when using OB70, YSU, and CMAQ Kv's from WRF/YSU.	13
Figure 3-5.	8 AM vertical profiles of Kv (top), ozone (middle), and NOx (bottom) at Hinton on June 9 from three CAMx runs using WRF/YSU meteorology (left) and the TCEQ base case using MM5 meteorology (right).	14
Figure 3-6.	2 PM vertical profiles of Kv (top), ozone (middle), and NOx (bottom) at Hinton on June 9 from three CAMx runs using WRF/YSU meteorology (left) and the TCEQ base case using MM5 meteorology (right).	16
Figure 3-7.	7 PM vertical profiles of Kv (top), ozone (middle), and NOx (bottom) at Hinton on June 9 from three CAMx runs using WRF/YSU meteorology (left) and the TCEQ base case using MM5 meteorology (right).	17
Figure 3-8.	Spatial plots of daily maximum 1-hour ozone on June 9 when using WRF/MYJ meteorology with different vertical diffusivity inputs (top row, bottom left), and using TCEQ base case inputs (bottom right).	19
Figure 3-8	(concluded). Spatial plots of daily maximum 1-hour ozone on June 9 when using WRF/MYJ meteorology with different vertical diffusivity inputs.	20
Figure 3-9.	Time series of hourly Kv's (top), ozone (middle), and NOx (bottom) from CAMx layer 1 at Denton when using OB70, YSU, CMAQ, TKE, and MYJ Kv's from WRF/MYJ.	21
Figure 3-10.	Time series of hourly Kv's (top), ozone (middle), and NOx (bottom) from CAMx layer 1 at Grapevine when using OB70, YSU, CMAQ, TKE, and MYJ Kv's from WRF/MYJ.	22
Figure 3-11.	Time series of hourly Kv's (top), ozone (middle), and NOx (bottom) from CAMx layer 1 at Hinton when using OB70, YSU, CMAQ, TKE, and MYJ Kv's from WRF/MYJ.	23
Figure 3-12.	8 AM vertical profiles of Kv (top), ozone (middle), and NOx (bottom) at Hinton on June 9 from five CAMx runs using WRF/MYJ meteorology	

meteorology (left) and the TCEQ base case using MM5 meteorology (right).	26
Figure 3-13. 2 PM vertical profiles of Kv (top), ozone (middle), and NOx (bottom) at Hinton on June 9 from five CAMx runs using WRF/MYJ meteorology (left) and the TCEQ base case using MM5 meteorology (right).	27
Figure 3-14. 7 PM vertical profiles of Kv (top), ozone (middle), and NOx (bottom) at Hinton on June 9 from five CAMx runs using WRF/MYJ meteorology (left) and the TCEQ base case using MM5 meteorology (right).	28
Figure 3-15. 7 PM vertical profiles of Kv (top), ozone (middle), and NOx (bottom) at Eagle Mountain Lake on June 9 from five CAMx runs using WRF/MYJ meteorology.	30

Executive Summary

Vertical turbulent mixing within the atmospheric boundary layer plays a crucial role in determining pollutant concentrations. Many environmental factors influence the onset, strength, depth, and duration of vertical mixing, making this process often one of the key sources of uncertainty and sensitivity in photochemical dispersion models. The TCEQ uses the Comprehensive Air quality Model with extensions (CAMx) to simulate the dispersion, chemistry and fate of ozone and precursors, and now uses the Weather Research and Forecasting (WRF) model to develop meteorological inputs for CAMx. The WRFCAMx meteorological interface program includes several user-selected algorithms for diagnosing vertical diffusivity (K_v) fields from WRF model outputs. An optional program called KVPATCH is often employed to further manipulate the K_v output from WRFCAMx to improve the turbulent coupling between the surface and the lower boundary layer.

The purpose of this Work Order was to update the techniques used to represent vertical mixing processes in CAMx. Various boundary layer schemes in WRF were analyzed and considered for implementation into the WRFCAMx interface program. CAMx model sensitivity to revised K_v inputs was conducted and analyzed. Eight CAMx sensitivity tests were performed for the June 7 – 10 period of the DFW 2006 ozone episode to evaluate the performance of two new vertical diffusivity methods: one based on the Yonsei University (YSU) bulk boundary layer scheme and the other based on the Mellor-Yamada-Janic (MYJ) turbulent kinetic energy (TKE) scheme. Three different diffusivity fields were computed from a WRF run with the YSU PBL scheme (OB70, CMAQ, YSU). Five diffusivity fields were computed from a WRF run with the MYJ PBL scheme (OB70, CMAQ, YSU, TKE, MYJ).

In the daytime, OB70 typically generated the lowest K_v 's and highest ozone and NO_x while CMAQ typically generated the highest vertical diffusivities, but lowest surface ozone and NO_x . All other methods fell between these two bounds. At night, surface layer diffusivities from OB70 usually increased while those from all other methods dropped rapidly, causing OB70 to mix out more surface NO_x and destroy less surface ozone via titration (all in better agreement with observed concentrations).

The YSU scheme, which was considered a replacement for OB70, did not perform well in the evenings. YSU and CMAQ were typically the first schemes to drop surface layer K_v 's below the critical value of $1 \text{ m}^2/\text{s}$ in the evening. This often led to very strong ozone and NO_x vertical gradients as excessive levels of NO_x were confined to layer 1, thereby speeding up ozone titration. This could pose a problem when simulating ozone if the daily maximum 8-hour ozone spanned one or more of the evening hours.

MYJ surface layer diffusivities were very close to the original TKE approach except in the daytime, when they were smaller. However, there was sufficient low-level mixing in the daytime from both methods that ozone results were very similar throughout the period.

A "patching" program should still be considered for all diffusivity methods to help control low-level K_v 's at night. We provide several recommendations for future work in this regard.

1.0 Introduction

Vertical turbulent mixing within the atmospheric boundary layer plays a crucial role in governing the spatial and temporal evolution of pollutant concentrations. Many environmental factors influence the onset, strength, depth, and duration of vertical mixing, including: atmospheric stability, rate of surface heating/cooling, type of surface cover, and the presence and character of cloud cover, among others. Vertical mixing is often one of the key sources of uncertainty and sensitivity in photochemical dispersion models.

The TCEQ uses the Comprehensive Air quality Model with extensions (CAMx) to simulate the dispersion, chemistry and fate of ozone and precursors. This photochemical modeling is central to State Implementation Plans for Texas ozone non-attainment areas. After years of employing Version 5 of the Mesoscale Model (MM5; Grell et al., 1995) to develop meteorological input data for CAMx, the TCEQ now uses the Weather Research and Forecasting (WRF; Skamarock et al., 2008) model for this purpose. The WRFCAMx meteorological interface program converts WRF output to CAMx input and is responsible for generating the vertical mixing rates (K_v) used in CAMx. WRFCAMx includes several user-selected algorithms for diagnosing K_v from WRF model outputs. An optional program called KVPATCH is often employed to further manipulate the K_v output from WRFCAMx to improve the turbulent coupling between the surface and the lower boundary layer. For example, enhanced vertical mixing over urban areas due to heat island and mechanically induced turbulence can be accounted for by applying landuse dependant K_v adjustments with the KVPATCH program.

The purpose of this Work Order was to update the techniques used to represent vertical mixing processes in CAMx. Various boundary layer schemes in WRF were analyzed and considered for implementation into the WRFCAMx interface program. CAMx model sensitivity to revised K_v inputs was conducted and analyzed. Based upon these results, new or revised options for the KVPATCH program are considered for future work.

1.1 APPROACH

The MM5CAMx and WRFCAMx programs prepare CAMx-ready meteorological fields from WRF. Both provide several options for computing vertical diffusivity (K_v) fields including: the O'Brien (1970) profile method (OB70), the K-theory method used in the Community Multi-scale Air Quality (CMAQ) model (Byun and Schere, 2006), the turbulent kinetic energy (TKE) method of Mellor and Yamada (1982), and the Asymmetric Convective Model (ACM2) of Pleim (2007). While these result in widely varying K_v fields during daytime hours, they often produce very low vertical diffusivities in the lowest model layers at night and early morning, excessively trapping urban NO_x in the lowest layers, resulting in too much ozone titration at night or inhibited ozone production in the morning. In past work, various K_v patches have been applied in the lowest model layers to enhance the vertical mixing of surface NO_x at night.

In this work, two planetary boundary layer (PBL) schemes used in WRF were reviewed to examine their computation of vertical diffusivities. The two routines reviewed were the Mellor-Yamada-Janic (MYJ) TKE scheme, and the Yonsei University (YSU) bulk boundary layer scheme. These algorithms were added into WRFCAMx and are described in more detail in Section 2.

CAMx vertical diffusivity fields were generated using these two new methods, in addition to the existing options, from two sets of WRF outputs provided by TCEQ. A 4-day period within the TCEQ Dallas-Fort Worth (DFW) 2006 episode (June 7-10, 2006) was used to evaluate impacts to simulated ozone and NO_x using the various Kv options. The MYJ approach was compared to the current WRFCAMx TKE option, and the YSU approach was considered as a possible replacement for the OB70 option. External Kv patches were not applied to any of these runs so that we could discern differences in low-level vertical mixing. An analysis of the impacts from the different vertical diffusivities in CAMx is discussed in Section 3. Findings and recommendations to further improve the Kv fields are discussed in Section 4.

2.0 Review of Two PBL Schemes in WRF

ENVIRON reviewed two PBL schemes used in WRF (v3.2.1 of the Advanced Research WRF [ARW] core) to examine the computation of vertical diffusivities. The two routines reviewed were the MYJ TKE scheme, and the YSU bulk boundary layer scheme.

2.1. YSU PBL SCHEME

The YSU approach (PBL physics option 1 in WRF) is a first-order K-theory scheme based on non-local boundary layer vertical diffusion. The original form of the YSU diffusion equation is

$$\frac{dC}{dt} = \frac{d}{dz} \left[K \left(\frac{dC}{dz} - \gamma \right) \right]$$

where C represents any prognostic variable, K is the eddy diffusivity coefficient, and γ is the correction to the local gradient. The latter accounts for large scale eddy contributions to the total flux, and has been found to generate more realistic daytime boundary layer structures (Hong and Pan, 1996). This version was employed in the operational Medium Range Forecast (MRF) model and later implemented as the “MRF” PBL option in MM5. The vertical diffusivity coefficients are computed by first finding the PBL height and then applying a stability profile function across the depth of the PBL.

In the YSU PBL implementation into WRF in 2004 (Hong et al., 2006), an additional term was added to the diffusion equation:

$$\frac{dC}{dt} = \frac{d}{dz} \left[K \left(\frac{dC}{dz} - \gamma \right) - \overline{(w'c')}_h \left(\frac{z}{h} \right)^3 \right]$$

where $\overline{(w'c')}_h$ presents the turbulent flux at the PBL top h , and z is the height of each layer. The extra term represents the explicit treatment of entrainment processes through the top of the PBL, which was found to help reduce excessive mixing when wind shear was strong and to enhance the under predicted vertical mixing when convection was strong.

In the YSU scheme, vertical diffusivities within the PBL are computed by first finding the mixing layer depth and scaling to a profile function:

$$K = k * w_s * z \left(1 - \frac{z}{h} \right)^p * f(Pr_o, z, h)$$

where k is the von Karman constant ($=0.4$), w_s is the convective velocity scale, p is the profile shape exponent ($=2$), and Pr_o is the Prandtl number. In CAMx, the vertical diffusivity used to mix chemical constituents is taken to be the diffusivity for heat K_h . In meteorological models, the vertical diffusivity for momentum K_m is usually calculated first and then scaled to K_h by the Prandtl number. In the YSU scheme, they introduce a vertically-varying function of the Prandtl number $f(Pr_o, z, h)$ into the computation.

Above the PBL, a local diffusion scheme based on the Louis (1979) local K approach is used in which the vertical diffusivities are a function of the gradient Richardson number Ri_g , mixing length l , and wind shear:

$$K_{loc} = l^2 f(Ri_g) \left(\frac{dV}{dz} \right)$$

In the entrainment zone directly above the PBL, the vertical diffusivities are calculated by taking the geometric average of the local vertical diffusivity shown above and the diffusivity in the entrainment zone (K_{ent}), shown below, which is assumed to decrease exponentially with height above the PBL. K_{ent} assumes that the buoyancy flux at the PBL is 15 % of the surface heat flux. The entrainment rate is defined as

$$w_e = \frac{\overline{(w'\theta_v')}_h}{\Delta\theta_{vh}}$$

where $\overline{(w'\theta_v')}_h$ is heat flux at h and θ_v is virtual potential temperature. Vertical diffusivity in the entrainment zone is computed as

$$K_{ent} = \frac{-w_e}{\Delta z} e^{\left[\frac{(z-h)^2}{\delta^2} \right]}$$

where δ is the fractional thickness of the entrainment zone in relation to the PBL height.

Additional details can be found in Hong et al. (2006). The YSU PBL scheme includes its own implicit tri-diagonal solver within WRF to vertically mix winds, temperature, moisture, and tracers according to its enhanced diffusion equation. While it is possible to calculate CAMx diffusivity profiles following the YSU approach (K , K_{loc} , K_{ent}), CAMx solves the standard diffusion equation that lacks the γ and $\overline{(w'c')}_h$ terms that are unique to the YSU approach. Adding these additional terms to the CAMx diffusion solver is outside the scope of this study. Nevertheless, the YSU vertical diffusivity equations were implemented into WRFCAMx.

2.2. MYJ PBL SCHEME

WRFCAMx currently includes an option to compute vertical diffusivities derived from TKE fields output from WRF, which is based on the first-order Level 2.5 scheme of Mellor and Yamada (1982) with modifications by Helfand and Labraga (1988) to adjust for growing turbulence. Janjic (1990, 1994) retuned the Mellor-Yamada scheme and improved its ability to treat shallow convection, resulting in the Mellor-Yamada-Janjic (MYJ) PBL scheme (PBL physics option 2 in WRF).

In both TKE schemes, the vertical diffusivities are calculated as

$$K = l q S$$

where l is the mixing length, q is $\sqrt{2 TKE}$, and S is a stability function tied to Richardson number. The first two variables in the equation above are computed in an identical fashion in both MYJ and the TKE option in WRFCAMx. The stability function is dependent on a multitude of empirical constants determined in neutral conditions. These constants are used to compute several other complex intermediate variables that differ among the two TKE schemes. The values of these empirical constants also differ between the MYJ and WRFCAMx TKE algorithms so it is not clear how this drives differences among the two vertical diffusivity approaches. We have added the MYJ diffusivity option to WRFCAMx to examine the differences between the two TKE schemes using the TCEQ test dataset.

2.3 KVPATCH

In previous modeling exercises, the CAMx vertical diffusivity profiles have been altered or “patched” in the lowest model layers using the KVPATCH program. Usually the purpose of the patch is to increase K_v values nearest the ground to help mix out excessive NO_x concentrations that tend to build up during stable periods in the lowest CAMx layers. Un-patched K_v fields led to large over predictions for nighttime/morning NO_x in urban environments, which in turn caused large under predictions in ozone either because of too much titration or inhibition of ozone production during the late morning. Patches have been used to raise the nocturnal vertical diffusivity floor in urban areas, and to use the maximum diffusivity in lowest 100 m of each vertical column for all of layers below 100 (referred to as the “KV100” patch). The latter patch was applied to the diffusivities for the 1999 base year ozone SIP modeling for Dallas-Fort Worth. CAMx sensitivity tests using WRF with the YSU and MYJ PBL schemes were evaluated in Section 3 without any patches to determine if there still are benefits to K_v patching.

3. CAMx MODELING

3.1. CAMX INPUTS

Two sets of WRF runs were obtained from TCEQ to evaluate sensitivities to the new vertical diffusivity methods introduced into the WRFCAMx converter. One WRF run was configured with the YSU PBL scheme and the other with the MYJ PBL scheme. Both runs covered the DFW May 31 to July 2, 2006 ozone modeling period and were configured with 2-way nesting for the 36 km and 12 km domains, and 1-way nesting for the 4 km domain.

The CAMx vertical diffusivity sensitivity tests reported here focused on the June 7 – 10 period, when 1 and 8-hour ozone measured 115 and 107 ppb, respectively, at the Denton monitoring site on June 9. All CAMx input files for the 2006 DFW base case were downloaded from <http://www.tceq.texas.gov/airquality/airmod/data/dfw8h2> in the original TCEQ Lambert projection (center at 40°N, 100°W with true latitudes at 30°N and 60°N). The DFW base case was first rerun using CAMx version 5.20.1 from May 31 to June 10 to ensure that it could be replicated. The CAMx restart files ending on June 6 were then used to begin all vertical diffusivity sensitivity tests.

The base case meteorological files were based on MM5, which employed the MRF PBL in the 36 and 12 km domains (early precursor to WRF's YSU), and the ETA PBL in the 4 km domain (MM5's TKE scheme). The MM5CAMx ACM2 vertical diffusivity option was used to generate Kv fields for the 36 and 12km domains, while the TKE option was used for the 4 km domain. A "KV200" patch was applied to the 4 km gridded diffusivities that sets all values in the lowest 200 m of each vertical column to the largest diffusivity found within that depth. TCEQ elected to integrate vertical mixing in CAMx using the ACM2 diffusion solver, instead of the original K-theory solver; ACM2 enhances daytime convective mixing via non-local exchange.

For the sensitivity tests reported here, WRFCAMx was run for the June 7-10 period to generate two sets of CAMx meteorological inputs with eight versions of vertical diffusivity files. WRF with YSU PBL was used to generate Kv files for the 36, 12, and 4 km domains based on three methods -- CMAQ, OB70, and the newly implemented YSU vertical diffusion. The other five Kv files were based on WRF with MYJ PBL using CMAQ, OB70, YSU, the original TKE, and updated MYJ TKE. A 0.1 m²/s minimum Kv floor was applied all files. No Kv patches were applied.

In all of the sensitivity tests, the latest publicly released version of CAMx (v5.30) was used. The original K-theory diffusion solver was used in lieu of the more expensive ACM2 diffusion solver. Three CAMx runs used meteorological files extracted from WRF with YSU PBL that varied only the three Kv files (CMAQ, OB70, YSU). Five CAMx runs used meteorological files extracted from WRF with MYJ PBL that varied only the five Kv files (CMAQ, OB70, YSU, TKE, MYJ). The two sets of WRF meteorology lead to different CAMx results because of differences in winds, temperatures, clouds, etc., beyond the differences in PBL models and Kv extractions. Likewise, these WRF outputs produce different CAMx results compared to the MM5-based meteorological fields used in the TCEQ base case run. We present some inter-comparisons using all three sets of meteorological inputs to illustrate their differences, but this evaluation is

not intended to determine which of the three meteorological configurations performs better. Instead, we focus on sensitivity to diffusivity from runs using the same meteorology.

3.2. CAMX RESULTS USING WRF WITH YSU PBL

During the June 7-10, 2006 period, the highest observed 1-hour ozone was 115 ppb at Denton on June 9. Figure 3-1 displays spatial plots of the daily maximum 1-hour ozone on June 9 in the DFW 4 km domain from the three Kv runs that used meteorology from WRF/YSU. For comparison, the daily maximum from the TCEQ base case is also included.

On June 9, the highest predicted ozone near DFW in all runs was located in Denton and Wise Counties. OB70 resulted in the highest daily maximum ozone while CMAQ yielded the lowest ozone with the ozone plume shifted westward away from Denton. The daily maximum ozone from the YSU run was usually in between OB70 and CMAQ.

In the next set of figures, time series are shown at selected sites to compare the three runs using WRF/YSU meteorology. Each figure shows time series of hourly vertical diffusivities at the top of layer 1, and ozone and NO_x concentrations within layer 1. Results from CMAQ are in green, OB70 in light blue, and YSU in dark blue. Three sites are shown: Denton and Grapevine represent locations with high observed ozone while Hinton represents a site in the urban core. Similar plots at all DFW ozone monitoring sites are provided in Appendix A.

Figure 3-2 shows time series at Denton, where the highest 1-hour ozone among all sites during the 4-day period was observed. Ozone was under predicted for most of the period in all three Kv runs. The CMAQ Kv's were the highest in the daytime, resulting in more vertical mixing and lower daytime ozone peaks. OB70 resulted in the lowest vertical mixing in the daytime and the highest ozone peaks, especially on June 8 and 9, which were the closest to the observed. YSU Kv's and ozone were usually in the middle of the three runs.

Unlike CMAQ and YSU, whose diurnal profiles of Kv were highest in the early afternoons, OB70 Kv's peaked in the evenings, which helped to mix out some of the NO_x and reduced ozone titration slightly. Nevertheless, NO_x was generally over predicted in the evenings and at night in all three runs, and ozone was under predicted. YSU did help reduce NO_x on the night of June 9, putting it in better agreement with the observations. During most other times, YSU tended to fall in between OB70 and CMAQ.

On June 9, Denton's observed ozone was highest at 4 PM. All three CAMx runs predicted peaks at 12 to 1 PM, suggesting that under predictions were more likely due to a different meteorological issue, perhaps in the wind field, so another site with high observed ozone -- Grapevine -- was evaluated (Figure 3-3). Grapevine observed a 1-hour ozone peak of 104 ppb on June 9 (95 ppb for 8-hour ozone). The three Kv profiles showed the same trend as at Denton. CMAQ had the highest vertical diffusivities in the daytime and the lowest ozone peaks. OB70 had the lowest Kv's in the daytime but the highest ozone, nearly matching the observed on the afternoon of June 9. YSU was again in the middle. At night, ozone was well under predicted in all three runs as NO_x in the evenings was over predicted. CMAQ predicted the

most NOx and lowest ozone; OB70 had higher Kv's in the evening hours, which helped mix out some NOx and reduce the titration of ozone.

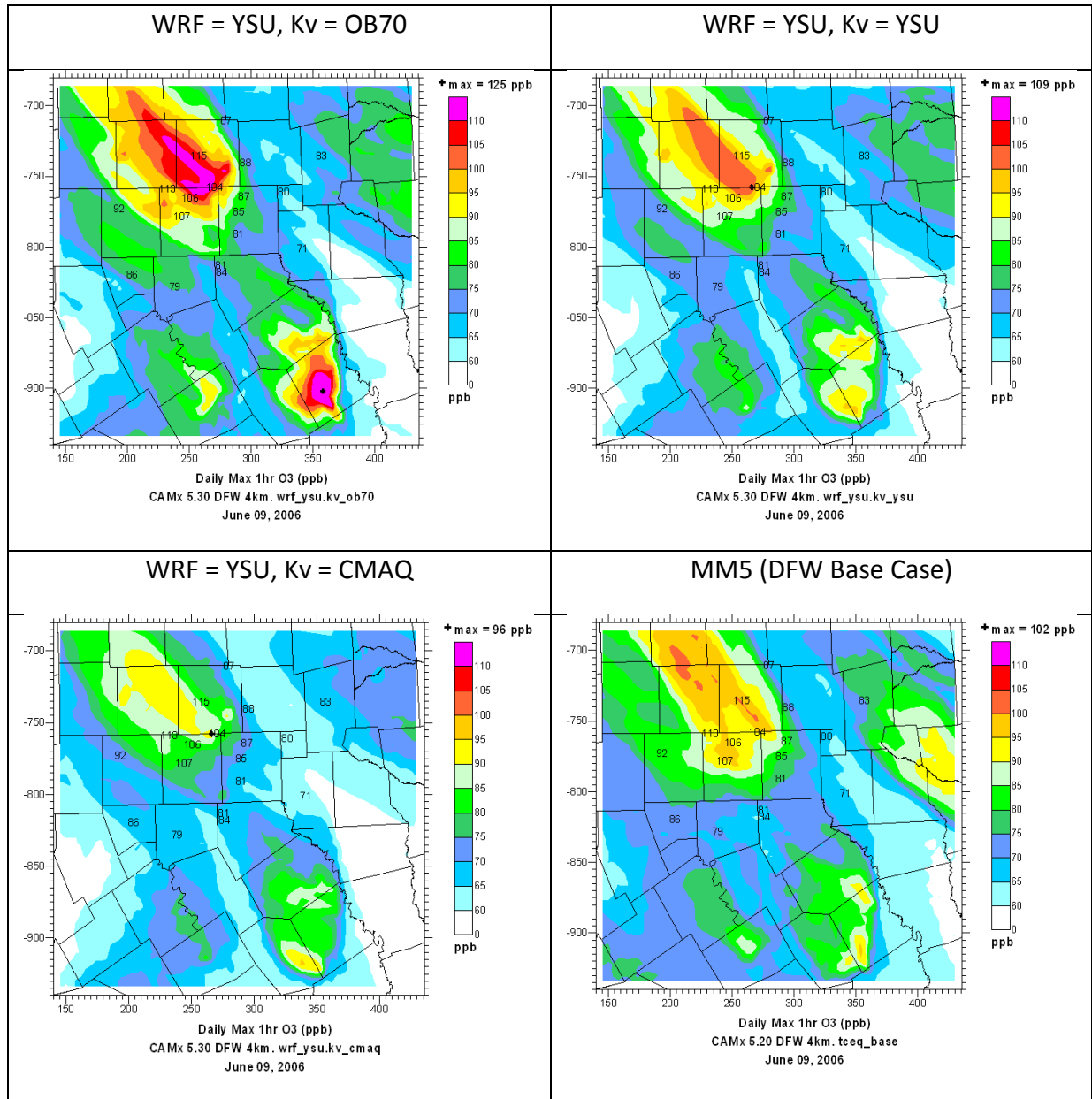


Figure 3-1. Spatial plots of daily maximum 1-hour ozone on June 9 when using WRF/YSU meteorology with different vertical diffusivity inputs (top row, bottom left), and using TCEQ base case inputs (bottom right).

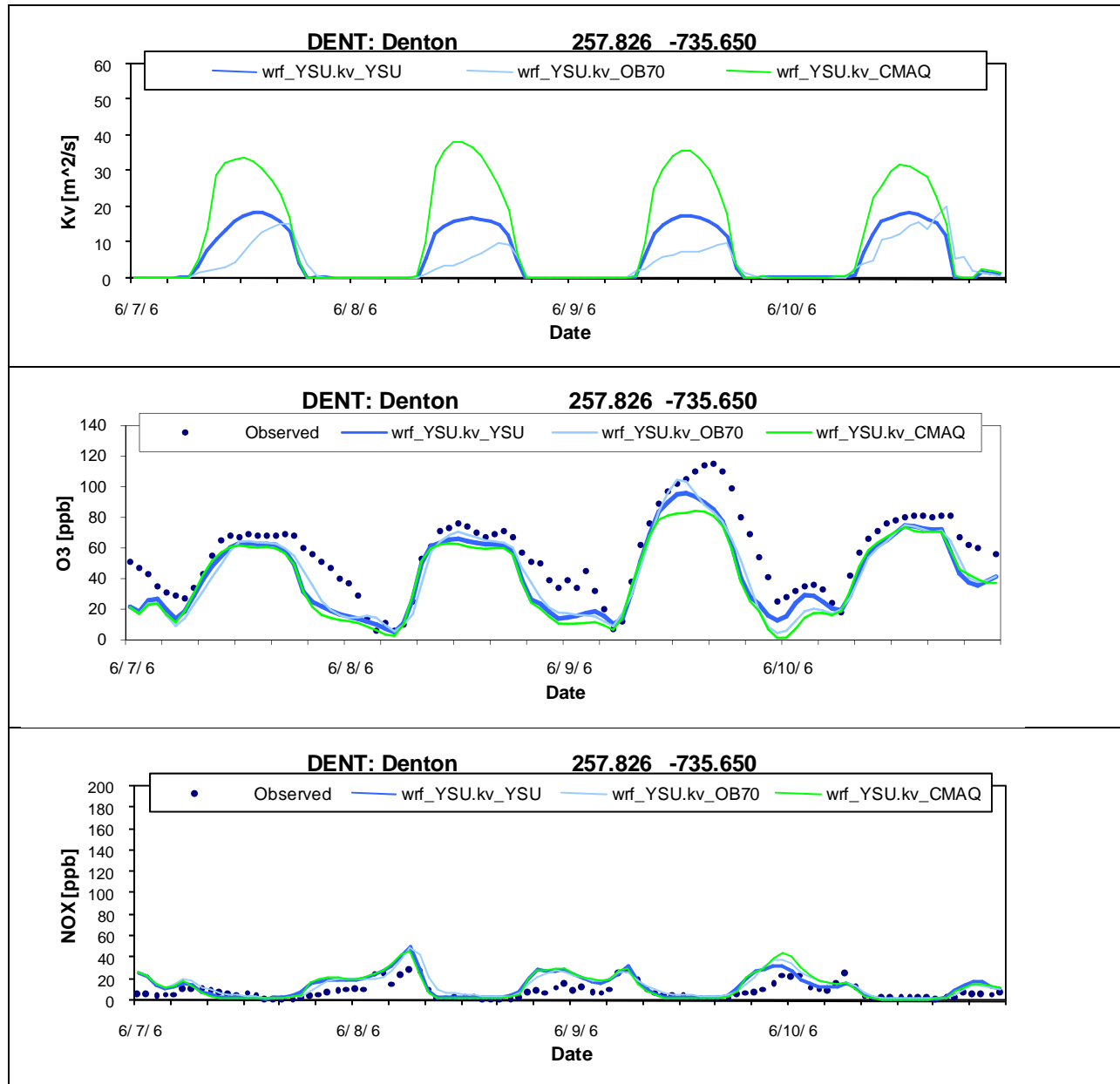


Figure 3-2. Time series of hourly Kv's (top), ozone (middle), and NOx (bottom) from CAMx layer 1 at Denton when using OB70, YSU, and CMAQ Kv's from WRF/YSU.

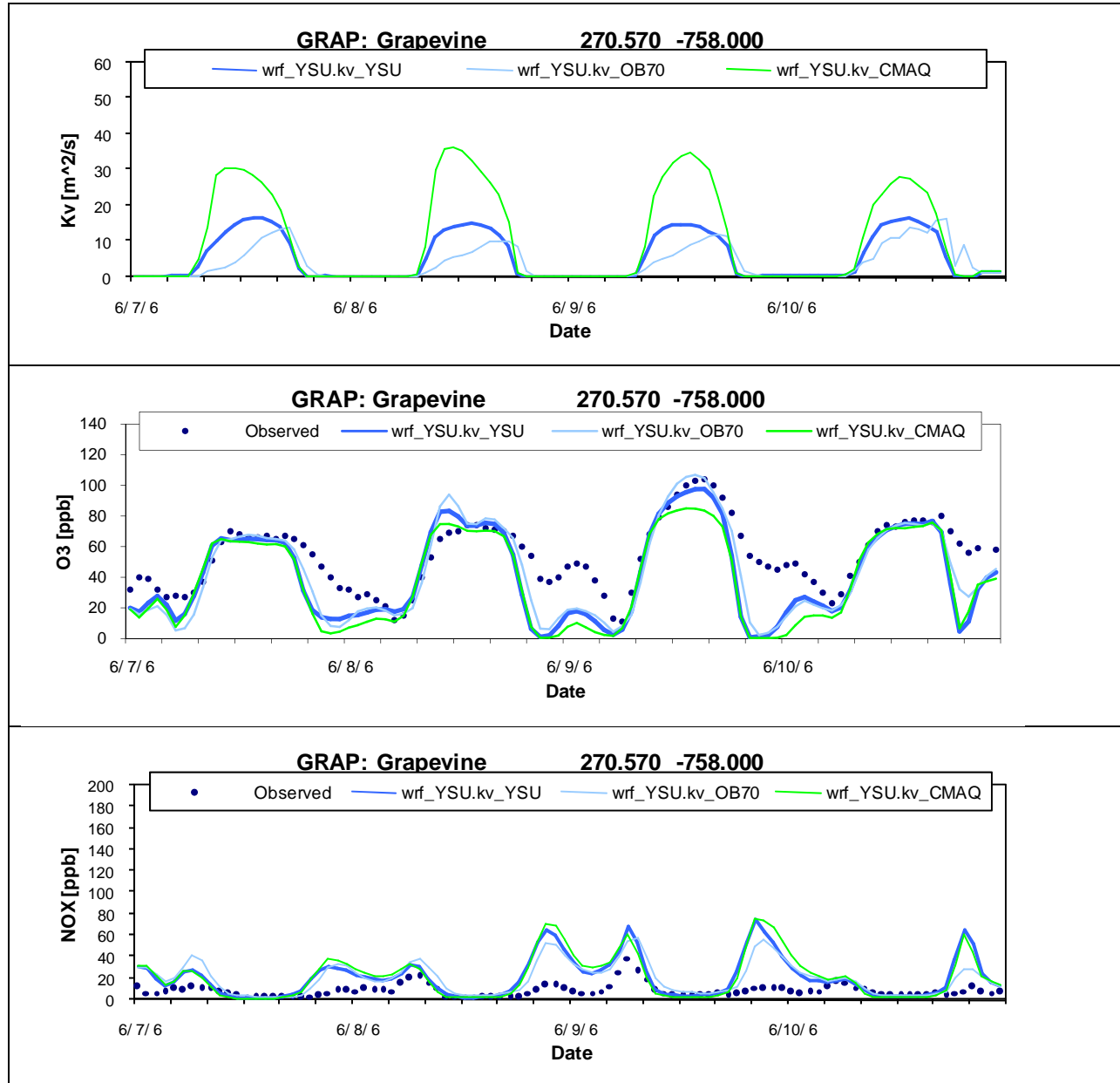


Figure 3-3. Time series of hourly Kv's (top), ozone (middle), and NOx (bottom) from CAMx layer 1 at Grapevine when using OB70, YSU, and CMAQ Kv's from WRF/YSU.

The third site – Hinton – represents the urban core and its time series are shown in Figure 3-4. The highest 1-hour ozone observed during this period was 85 ppb on June 9. CMAQ vertical diffusivities were again the highest in the daytime. YSU and OB70 Kv's were comparable in magnitude, but YSU was always highest in the early afternoon while OB70 was highest in the evening. At night, OB70 Kv's were the highest of the three.

All three CAMx runs predicted daytime ozone concentrations pretty close to one another except on June 9 when CMAQ predicted noticeably less ozone. From the evening to early morning hours, both YSU and CMAQ Kv's were very small (mostly between 0.1 and 0.3 m²/s); NOx was excessively trapped in layer 1, causing too much ozone titration in the evening hours. Ozone and NOx performance were much better in OB70 than CMAQ or YSU in the evenings because OB70 Kv's were higher (close to 1 m²/s before midnight). This suggests that the use of the landuse-based KVPATCH, in which a minimum Kv of 1 m²/s is set over urban areas, would continue to be beneficial to ozone performance for all three Kv methods as it helps mix out some of the low-level NOx, especially at night.

Vertical profiles of Kv, ozone, and NOx were generated at Hinton for three time periods on June 9: 8 AM when ozone production is starting, 2 PM when the highest ozone is observed, and 7 PM when the sun is setting and ozone titration begins. Figure 3-5 compares the vertical profiles at 8 AM for the three Kv runs. For comparison, similar vertical profiles from the DFW base case are also shown. CMAQ had the highest Kv's throughout the shallow mixed layer, YSU was in the middle, and OB70 had the lowest. With stronger vertical mixing there was less NOx and more ozone. Table 3-1 compares the surface Kv, ozone and NOx from the three runs at 8 AM. YSU matched the observed ozone at the surface, but slightly under predicted NOx. OB70 was closest to the observed NOx, but predicted too little ozone.

Compared to the TCEQ base case run with MM5 meteorology and the KV200 patch, WRF Kv's were smaller but WRF had a deeper mixed depth. The higher diffusivities in the base case mixed out more low-level NOx than in any of the WRF-based runs, and ozone was slightly over predicted. However, other meteorological factors may have contributed to these differences as well.

Table 3-1. Comparison of 8 AM layer 1 vertical diffusivities, ozone and NOx at Hinton when using WRF/YSU meteorology.

Kv Method	Kv (m ² /s)	Ozone [ppb]	NOx [ppb]
Observed	--	48	27
OB70	3.8	42	31
YSU	7.6	48	21
CMAQ	12.9	50	15

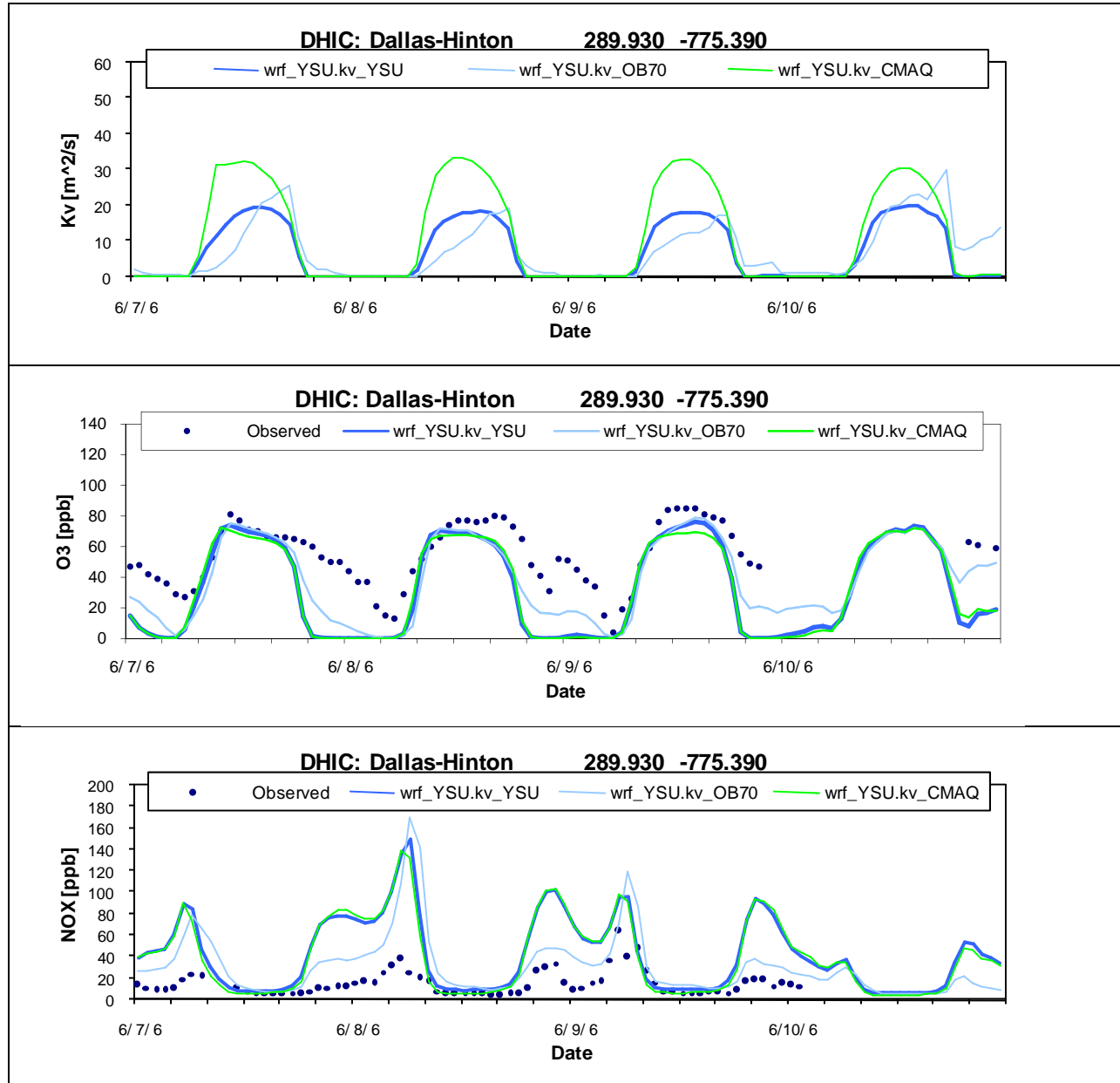


Figure 3-4. Time series of hourly Kv's (top), ozone (middle), and NOx (bottom) from CAMx layer 1 at Hinton when using OB70, YSU, and CMAQ Kv's from WRF/YSU.

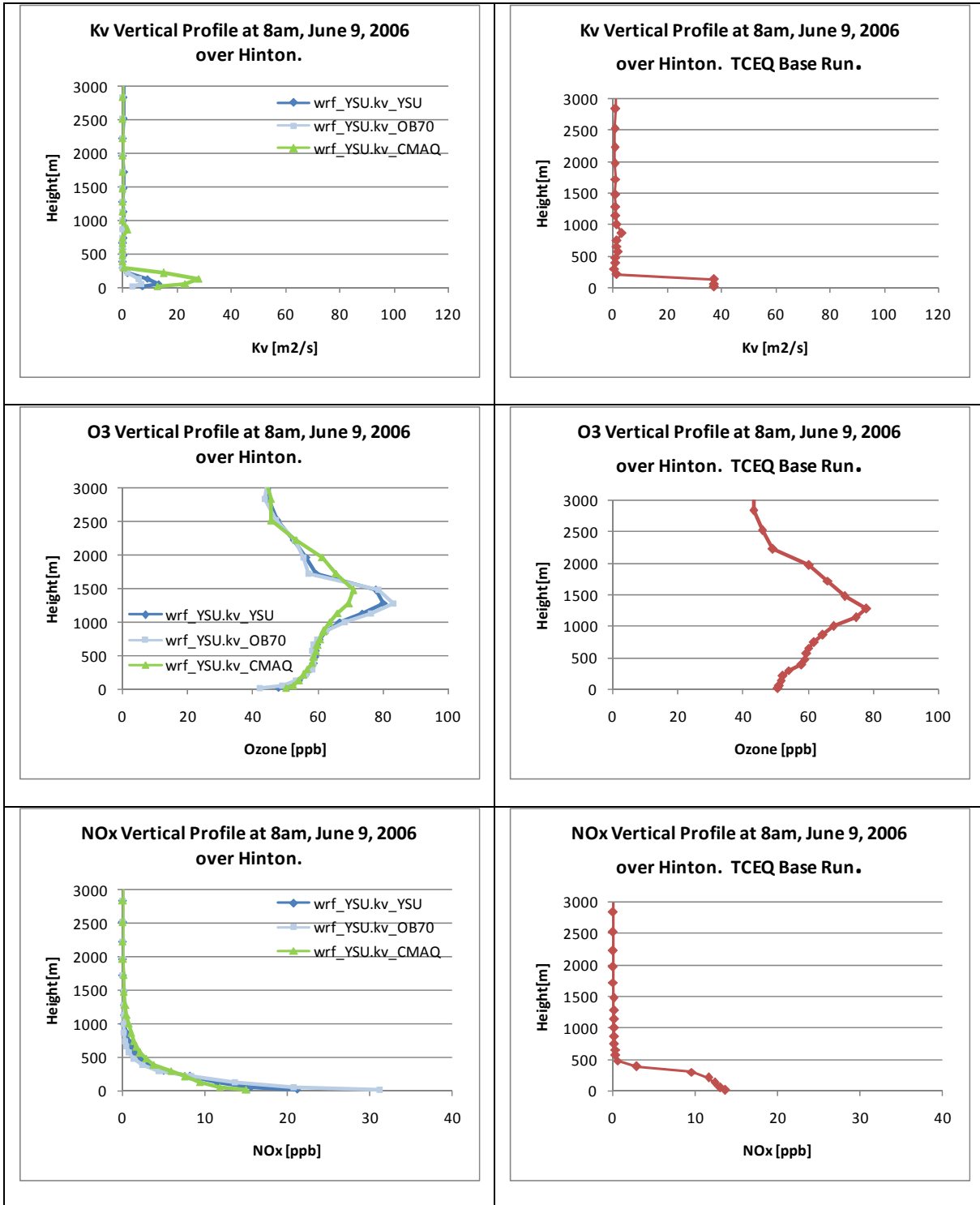


Figure 3-5. 8 AM vertical profiles of Kv (top), ozone (middle), and NOx (bottom) at Hinton on June 9 from three CAMx runs using WRF/YSU meteorology (left) and the TCEQ base case using MM5 meteorology (right).

Hinton vertical profiles of K_v , ozone, and NO_x at 2 PM on June 9, when the observed ozone was at its highest (85 ppb), are shown in Figure 3-6. Again, OB70 generated the lowest K_v 's, YSU was in the middle, and CMAQ had the largest values. The low mixing from OB70 resulted in the highest (but under predicted) ozone and NO_x at the surface, as can be seen in Table 3-2. YSU predicted slightly less ozone while CMAQ diluted ozone too much, but was closest to the observed in NO_x . Aloft, CMAQ averaged 10 ppb less ozone than OB70 in the lowest 1500 m. YSU predicted less ozone than OB70 at the surface, but their profiles are similar farther aloft. The MM5 meteorology used in the TCEQ base case generated a much shallower boundary layer with diffusivities on par with CMAQ; this combination led to surface ozone near the WRF OB70 and YSU results, surface NO_x closer to CMAQ, but a quicker fall off of ozone above 1500 m.

Table 3-2. Comparison of 2 PM layer 1 vertical diffusivities, ozone and NO_x at Hinton when using WRF/YSU meteorology.

Kv Method	Kv (m^2/s)	Ozone [ppb]	NO_x [ppb]
Observed	--	85	6
OB70	13.0	80	13
YSU	17.9	77	10
CMAQ	31.3	70	7

At 7 PM on June 9, the vertical diffusivity profiles from the three runs differed greatly, as can be seen in Figure 3-7. OB70 generated the highest K_v 's in layer 1 ($3.3 \text{ m}^2/\text{s}$), but all other layers were set to the minimum of $0.1 \text{ m}^2/\text{s}$. YSU and CMAQ generated more complex mixing layers aloft (300 to 800 m). The low CMAQ and YSU diffusivities in layer 1 confined too much NO_x to the lowest layer, resulting in too much ozone titration. Both runs predicted 4 times too much surface NO_x , which resulted in 51 ppb less ozone than observed (Table 3-3). This is in sharp contrast to layer 2, where ozone was 46 ppb higher than in layer 1 and NO_x was 63 ppb (or ~ 7 times smaller) than in layer 1. The OB70 run fared better, but ozone was still half of observed and NO_x was twice observed, as OB70 was able to spread its ozone and NO_x over two layers whereas CMAQ and YSU confined concentrations to one layer.

This suggests that K_v patches are still needed for all of these diffusivity methods, especially one that will boost layer 1 K_v to mix out surface NO_x and slow down ozone titration in the evenings. The K_v patch that sets the minimum to $1 \text{ m}^2/\text{s}$ over urban areas would have helped. The KV100 (or KV200) patch would have increased the low-level diffusivities for the CMAQ and OB70 profiles, but would have benefitted YSU only if the landuse-based patch had also been applied because the near-surface diffusivities in the YSU profile were all below $1 \text{ m}^2/\text{s}$. In the TCEQ base case, near-surface diffusivities were significantly higher than any of the WRF-based K_v 's and show a 500 m deep mixed layer at 7 PM. As a result, low-level ozone and NO_x was much closer to observations. However, it is uncertain whether other meteorological variables affected that outcome.

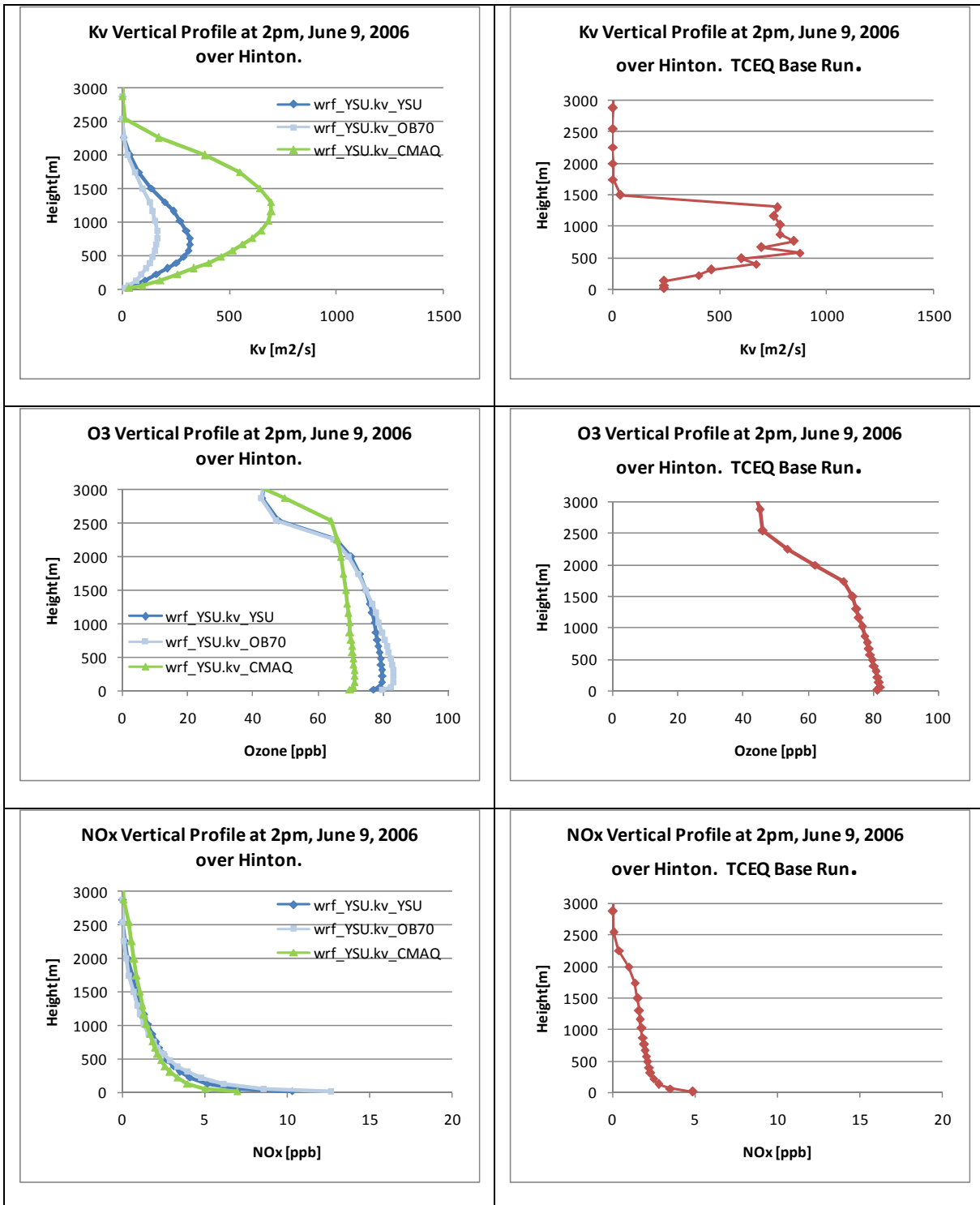


Figure 3-6. 2 PM vertical profiles of Kv (top), ozone (middle), and NOx (bottom) at Hinton on June 9 from three CAMx runs using WRF/YSU meteorology (left) and the TCEQ base case using MM5 meteorology (right).

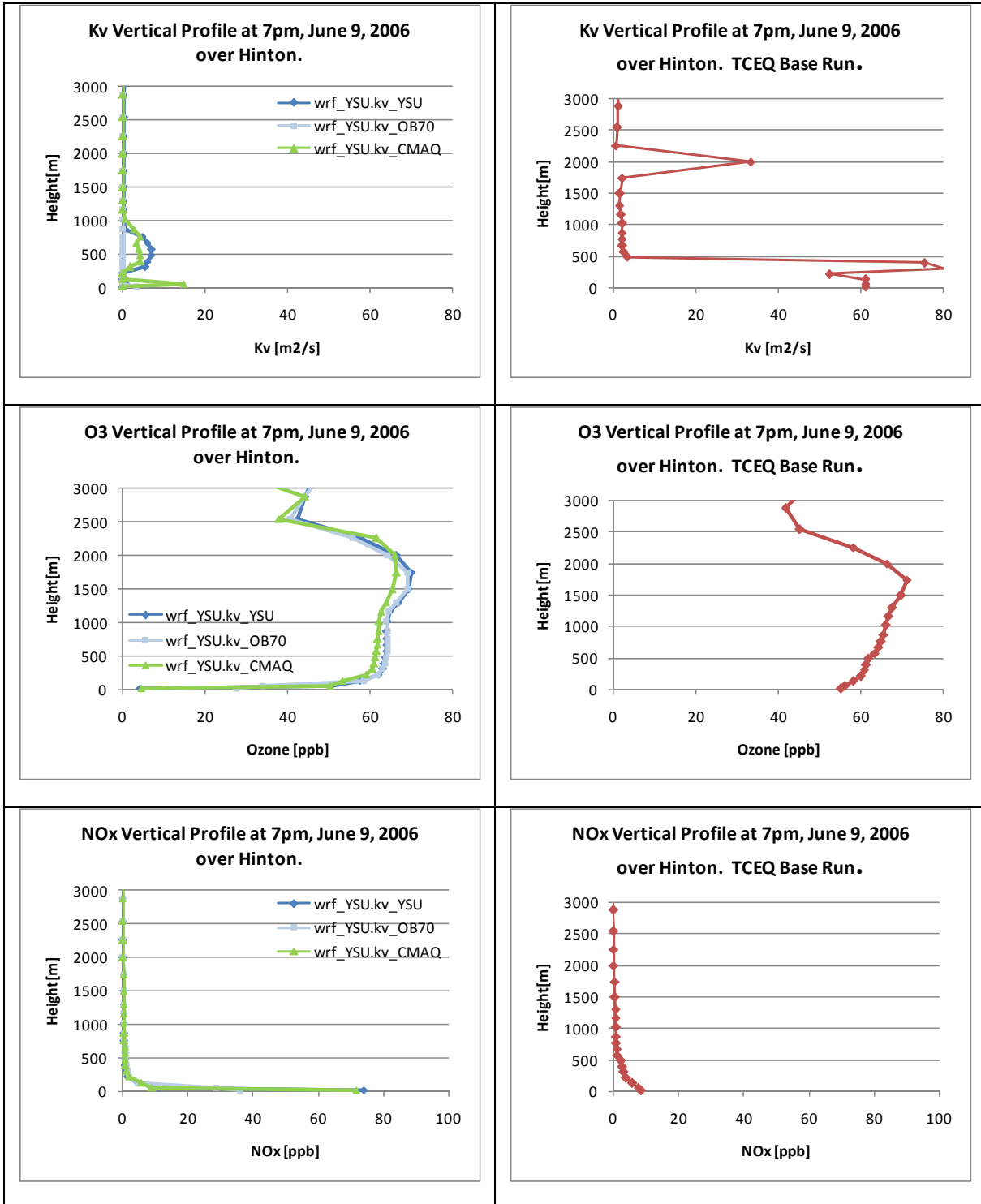


Figure 3-7. 7 PM vertical profiles of Kv (top), ozone (middle), and NOx (bottom) at Hinton on June 9 from three CAMx runs using WRF/YSU meteorology (left) and the TCEQ base case using MM5 meteorology (right).

Table 3-3. Comparison of 7 PM layer 1 vertical diffusivities, ozone and NOx at Hinton when using WRF/YSU meteorology.

Kv Method	Kv (m ² /s)	Ozone [ppb]	NOx [ppb]
Observed	--	55	17
OB70	3.3	27	36
YSU	0.1	4	74
CMAQ	0.1	4	72

3.3. CAMX RESULTS USING WRF WITH MYJ PBL

Figure 3-8 compares spatial plots of daily maximum 1-hour ozone on June 9 using the five different Kv methods derived from WRF/MYJ meteorology. As with the WRF/YSU meteorology, OB70 produced the highest ozone and CMAQ the lowest, where in the latter case the plume of high ozone was west of Denton. YSU was again in the middle. The daily maximum ozone in Denton and Wise Counties was higher with the MYJ PBL scheme than the YSU PBL scheme in each of the three corresponding Kv methods. The two TKE methods do not exhibit many differences in the daily maximum spatial plots. Both predicted the area with the highest ozone would be further west than YSU or OB70, and in the same vicinity as CMAQ, and both of their ozone concentrations were slightly higher than the YSU method but lower than OB70.

Time series of hourly layer 1 vertical diffusivities, ozone and NOx concentrations are plotted in Figures 3-9 to 3-11 for the same three sites as shown previously (Denton, Grapevine, and Hinton, respectively). All five Kv sensitivity runs are displayed in each figure. At Denton, daytime Kv's were highest from the CMAQ and TKE methods. MYJ had the next highest each day, followed by YSU and then OB70. As Kv reduced, peak daytime ozone increased. OB70, with the lowest daytime Kv's, had the highest daytime ozone and was closest to observed. CMAQ had the lowest daytime ozone. YSU, TKE, and MYJ Kv's differed greatly in the daytime, but all were sufficiently large that they resulted in a well mixed boundary layer and similar ozone peaks over Denton. It should also be noted that the use of the MYJ scheme in WRF did not result in ozone peaks too early over Denton on June 9 as was the case when using the YSU PBL.

At night, all Kv's were low, but OB70 had the highest values. This helped mix out some of the low-level NOx and reduce ozone titration. Time series show ozone and NOx tracking the observed very well on the nights of June 7 and 8. On the night of June 9, OB70 Kv's may have been too high as NOx was under predicted and ozone was over predicted. YSU, with the second highest Kv's on that night, showed the best performance. CMAQ, TKE, and MYJ over predicted low-level NOx and had too much ozone titration on all nights as vertical mixing was minimal.

At Grapevine, the Kv time series showed the same trend as at Denton. CMAQ and TKE Kv's were the highest in the daytime, followed by MYJ, YSU, and OB70. All Kv's peaked in the early afternoon except for OB70, whose highest Kv always occurred in the evenings. Daytime ozone and NOx were highest with OB70 on June 8 and 9, and lowest with CMAQ. The two TKE showed similar ozone time series in the daytime over Grapevine, even though MYJ daytime Kv's were much smaller than TKE.

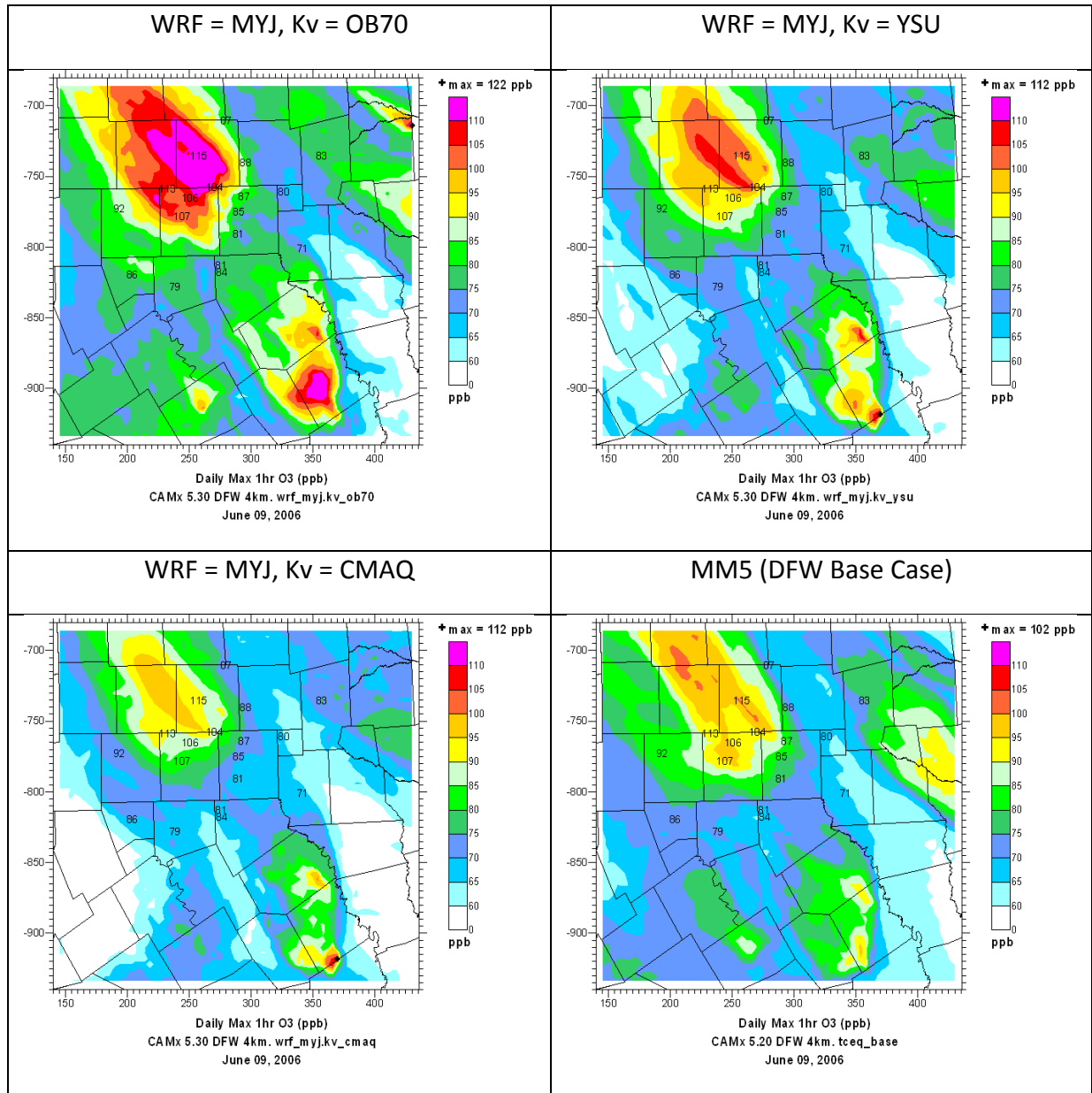


Figure 3-8. Spatial plots of daily maximum 1-hour ozone on June 9 when using WRF/MYJ meteorology with different vertical diffusivity inputs (top row, bottom left), and using TCEQ base case inputs (bottom right).

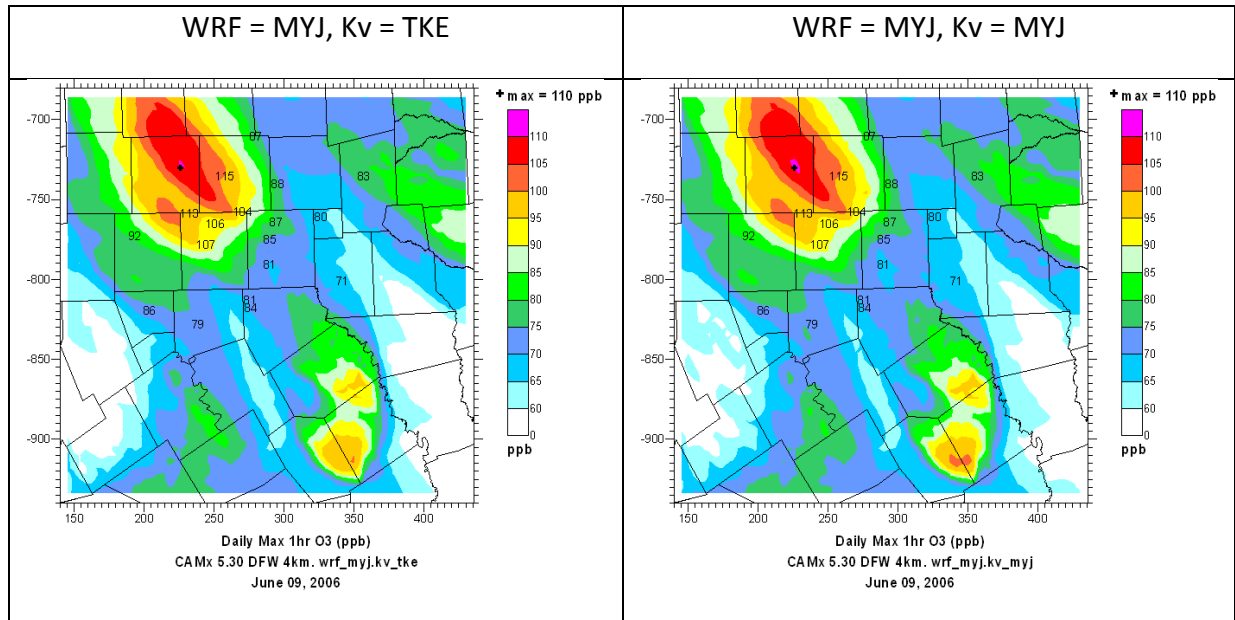


Figure 3-8 (concluded). Spatial plots of daily maximum 1-hour ozone on June 9 when using WRF/MYJ meteorology with different vertical diffusivity inputs.

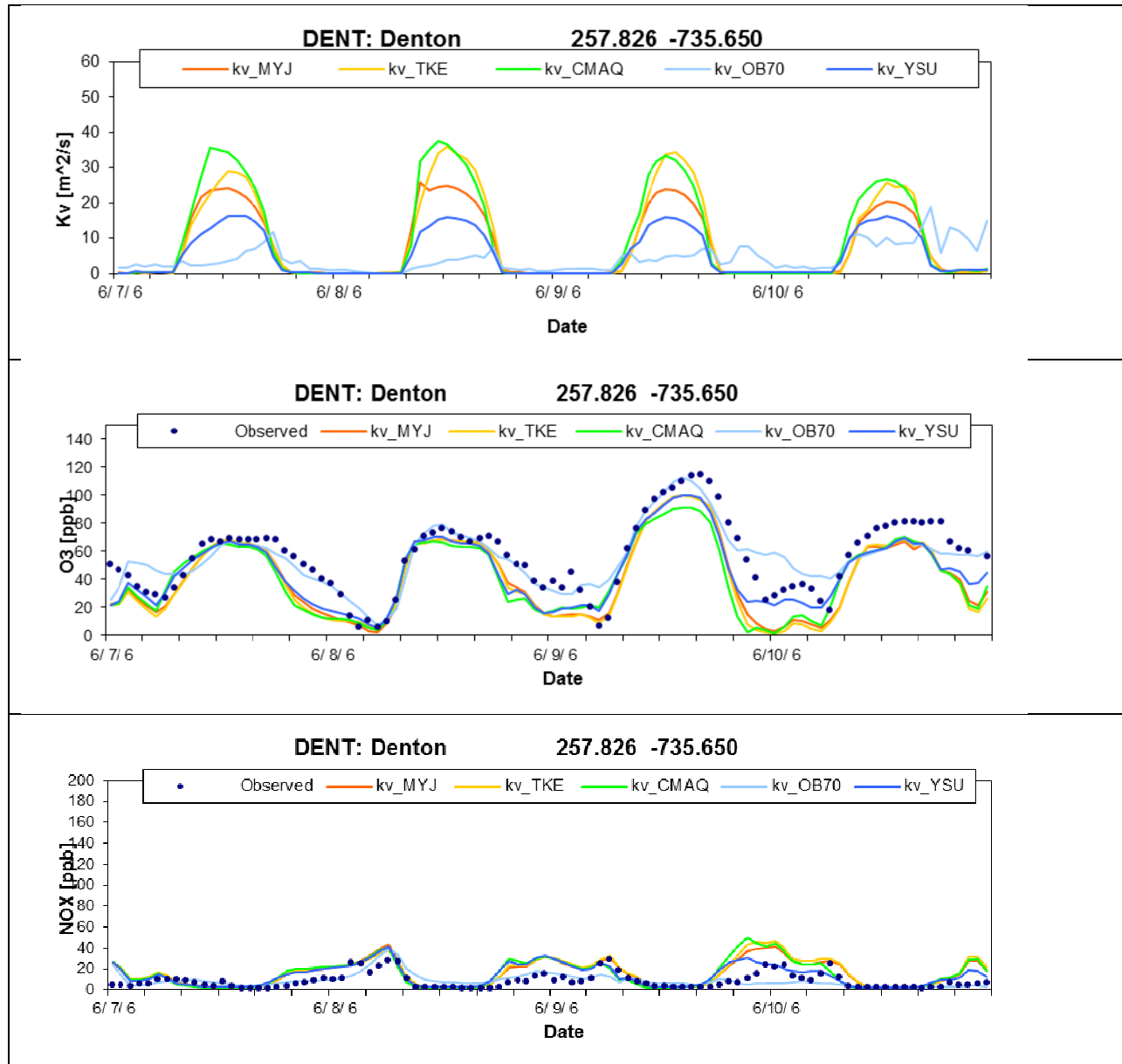


Figure 3-9. Time series of hourly Kv's (top), ozone (middle), and NOx (bottom) from CAMx layer 1 at Denton when using OB70, YSU, CMAQ, TKE, and MYJ Kv's from WRF/MYJ.

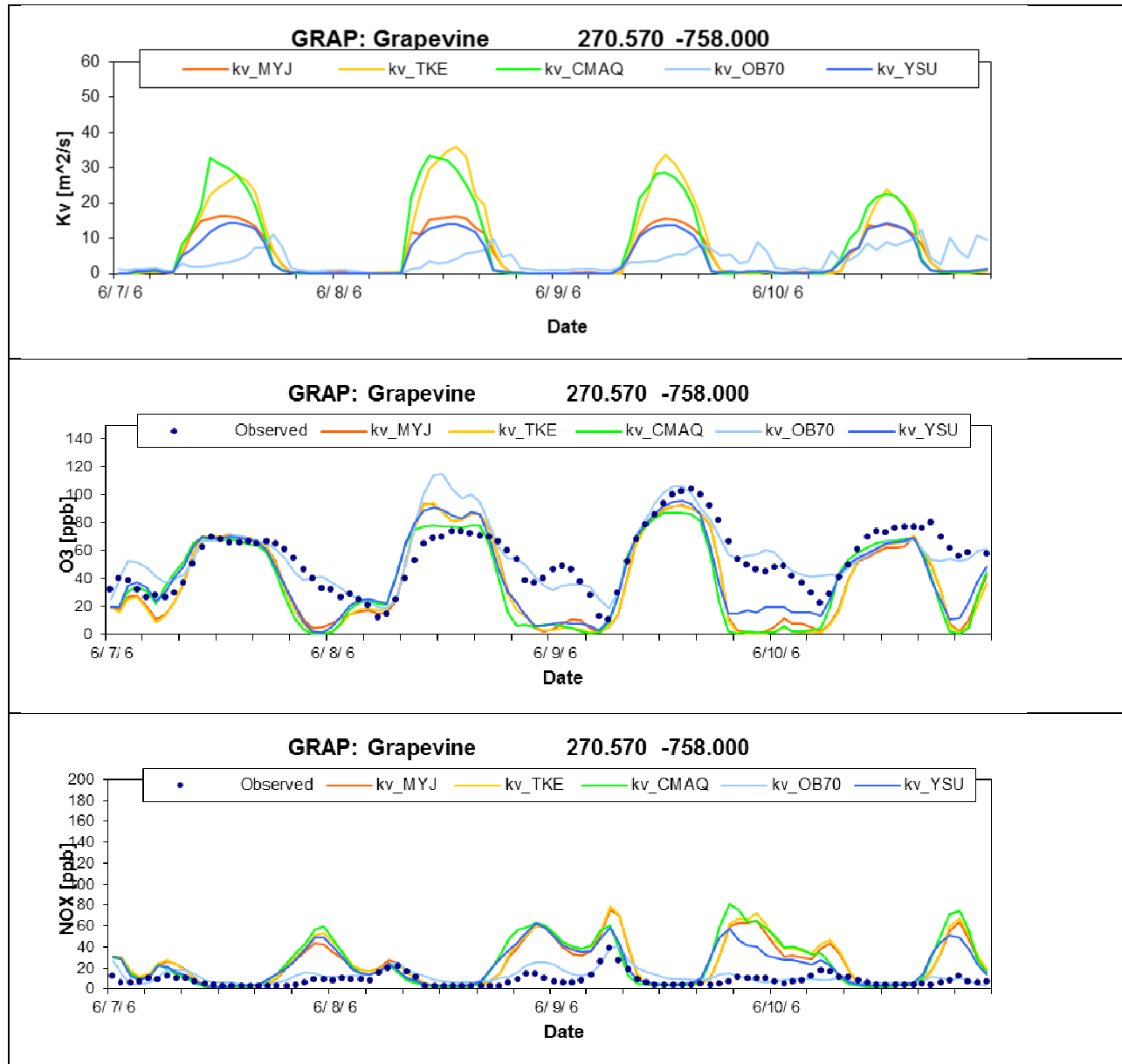


Figure 3-10. Time series of hourly K_v 's (top), ozone (middle), and NO_x (bottom) from CAMx layer 1 at Grapevine when using OB70, YSU, CMAQ, TKE, and MYJ K_v 's from WRF/MYJ.

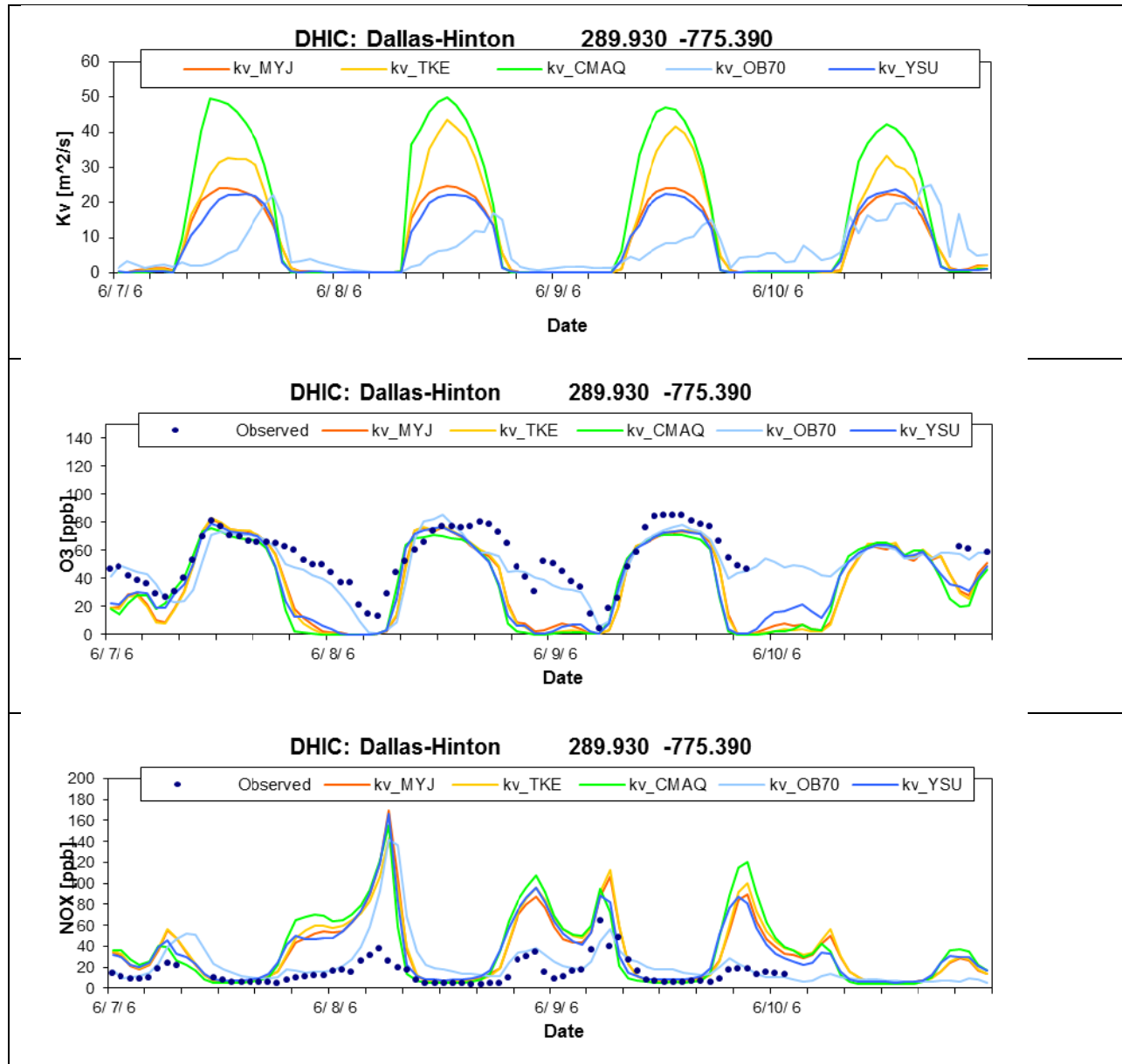


Figure 3-11. Time series of hourly Kv's (top), ozone (middle), and NOx (bottom) from CAMx layer 1 at Hinton when using OB70, YSU, CMAQ, TKE, and MYJ Kv's from WRF/MYJ.

At night, OB70 performed the best as it allowed more NO_x to mix out of layer 1, resulting in less ozone titration. The other four runs all had very low K_v's, resulting in over predictions in NO_x and under predictions in surface ozone. Vertical diffusivities from YSU and MYJ were relatively close to one another. In the evenings, the YSU K_v's tended to drop very low earlier than MYJ (and TKE), resulting in faster ozone titration. In the morning, YSU K_v's tended to grow faster than MYJ, helping increase ozone production. This trend can be seen at many sites besides Grapevine; similar time series for all DFW sites are available in Appendix B.

At Hinton, an ozone monitor in the urban core, daytime K_v's exhibited similar trends. CMAQ had the highest daytime values, followed by TKE, MYJ, YSU, and then OB70. The main exception was on June 10, when late afternoon OB70 K_v's were higher than either MYJ and YSU. Daytime ozone concentrations from the five runs were in a relatively tight range, but OB70 typically produced the highest daily peaks while CMAQ had the lowest. At night, OB70 showed the best surface ozone and NO_x performance since it had the highest K_v's, as seen at Denton and Grapevine. The other four methods resulting in K_v's that were too low at night, resulting in low vertical mixing of NO_x and faster-than-observed ozone titration.

Vertical profiles of K_v, ozone, and NO_x over the urban monitoring site – Hinton – are displayed at the same three times on June 9 as previously examined for the WRF/YSU case (Figures 3-12 through 3-14). At 8 AM, CMAQ resulted in the highest K_v's throughout the lowest 1000 m. In the lowest 350 m, YSU had the second highest K_v's in most layers, followed by OB70; the TKE and MYJ profiles were the lowest except in layer 1 (where OB70 was lowest). Above 350 m, MYJ K_v's were not nearly as large as those from the original TKE method. CAMx matched the 48 ppb observed ozone, and was within 2 ppb of observed NO_x (27 ppb) from the three runs with the lowest layer 1 K_v (OB70, TKE, and MYJ), as summarized in Table 3-4. The higher K_v's in the other methods led to under predictions of layer 1 NO_x, particularly from YSU and CMAQ.

Table 3-4. Comparison of 8 AM layer 1 vertical diffusivities, ozone and NO_x at Hinton when using WRF/MYJ meteorology.

K _v Method	K _v (m ² /s)	Ozone [ppb]	NO _x [ppb]
Observed	--	48	27
OB70	4.6	48	29
YSU	11.6	53	15
CMAQ	23.8	55	10
TKE	10.2	48	25
MYJ	10.1	48	25

At the 2 PM ozone peak, all five runs under predicted ozone at Hinton. OB70 had the highest surface ozone and NO_x (Table 3-5) because it had the weakest vertical mixing throughout the mixed layer. CMAQ exhibited the lowest ozone and NO_x since it had the strongest vertical mixing, although its 6 ppb NO_x did match the observed. YSU, TKE, and MYJ had similar ozone profiles in the lowest 1000 m, but low-level NO_x in the YSU case was higher than both TKE and MYJ (and the observed) due to its smaller K_v's. TKE and MYJ K_v's occasionally exceeded CMAQ K_v's from 350 to 1500m; the magnitudes are quite large so these differences did not result in

much change to their ozone profiles. Note that the WRF/MYJ run generated an equivalent PBL depth to the TCEQ base case run, which also utilized a TKE PBL treatment.

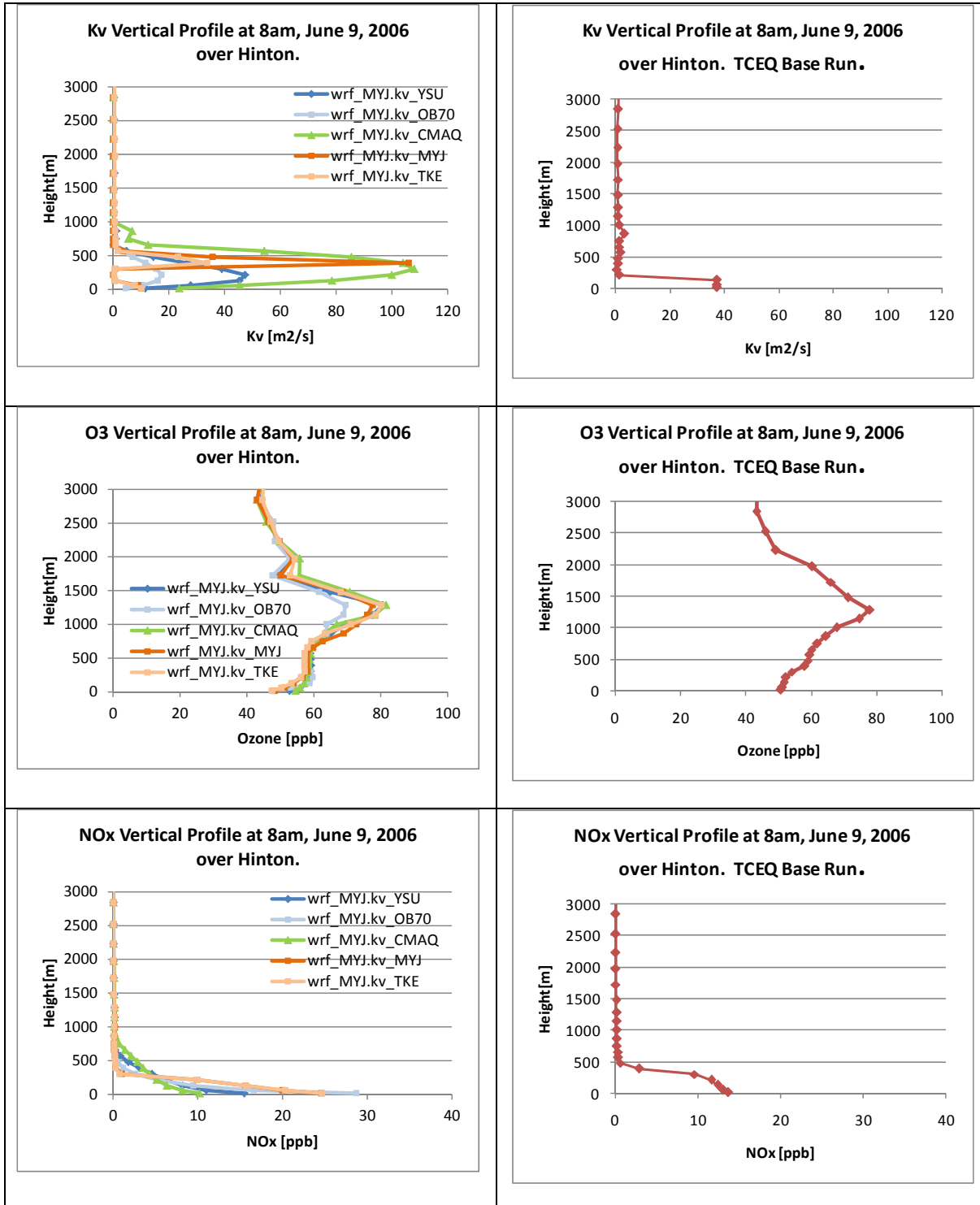


Figure 3-12. 8 AM vertical profiles of Kv (top), ozone (middle), and NOx (bottom) at Hinton on June 9 from five CAMx runs using WRF/MYJ meteorology meteorology (left) and the TCEQ base case using MM5 meteorology (right).

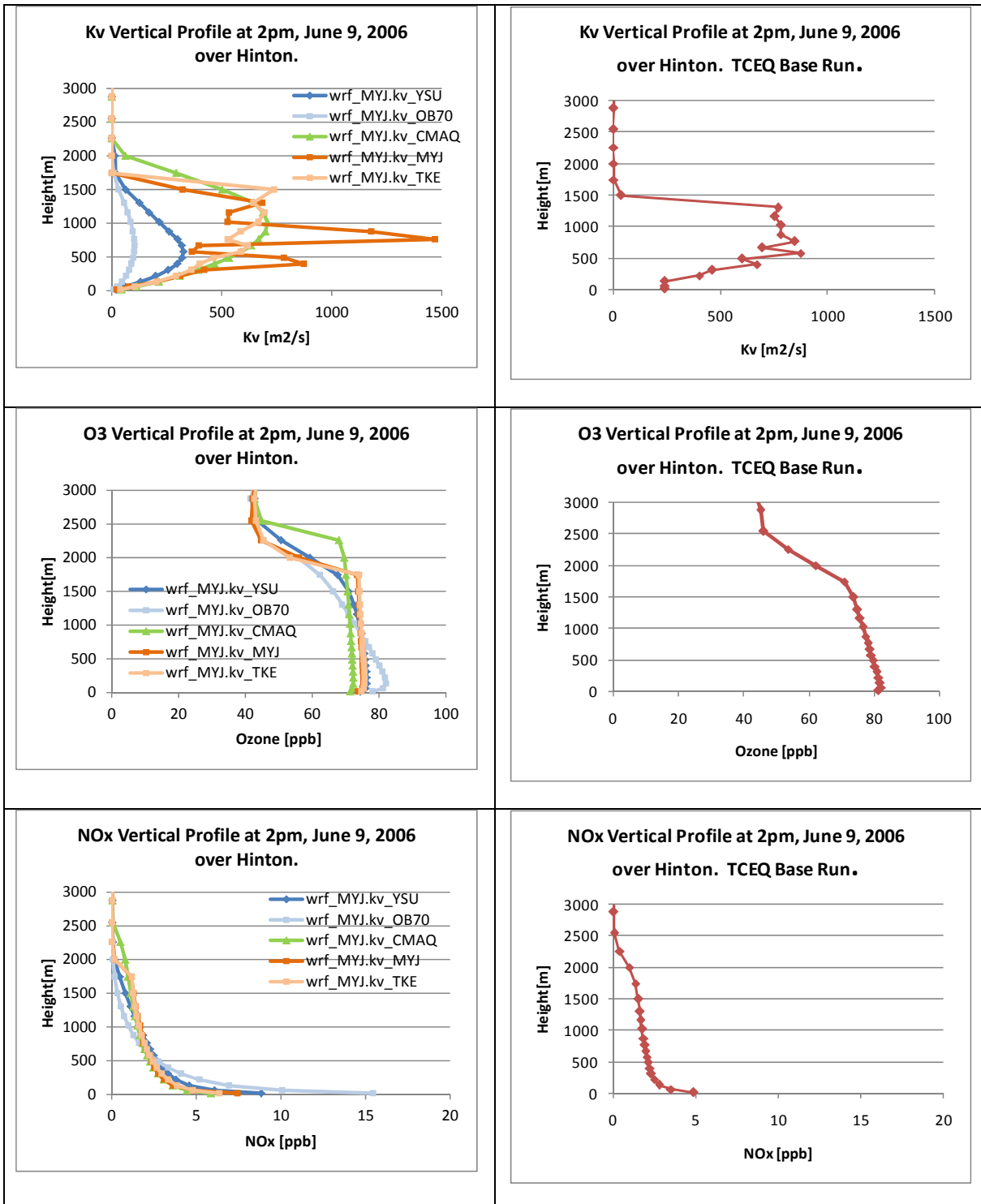


Figure 3-13. 2 PM vertical profiles of Kv (top), ozone (middle), and NOx (bottom) at Hinton on June 9 from five CAMx runs using WRF/MYJ meteorology (left) and the TCEQ base case using MM5 meteorology (right).

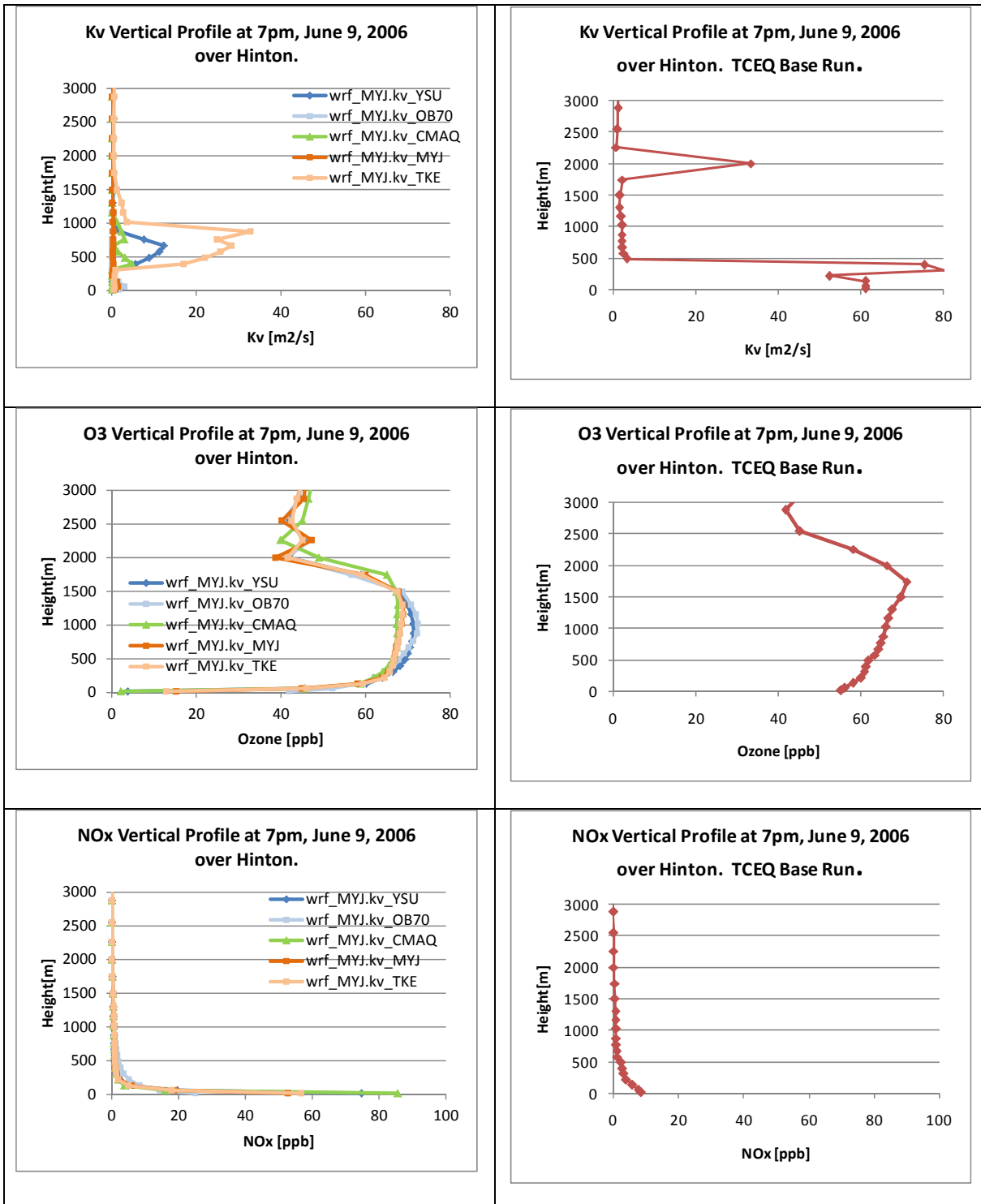


Figure 3-14. 7 PM vertical profiles of Kv (top), ozone (middle), and NOx (bottom) at Hinton on June 9 from five CAMx runs using WRF/MYJ meteorology (left) and the TCEQ base case using MM5 meteorology (right).

Table 3-5. Comparison of 2 PM layer 1 vertical diffusivities, ozone and NOx at Hinton when using WRF/MYJ meteorology.

Kv Method	Kv (m ² /s)	Ozone [ppb]	NOx [ppb]
Observed	--	85	6
OB70	9.9	78	15
YSU	21.7	74	9
CMAQ	43.7	71	6
TKE	39.7	75	6
MYJ	23.3	74	7

At 7 PM, CMAQ Kv's were at the 0.1 m²/s minimum for the first 5 layers (up to ~350 m); the lack of vertical mixing led to the buildup of NOx that was 5 times higher than observed and very strong ozone titration that reduced ozone to 2 ppb at a time when the observed ozone was 55 ppb (Table 3-6). YSU suffered a similar problem, although its diffusivities in the first five layers were slightly higher. OB70 Kv's, which were consistently higher at night near the surface, resulted in the best predictions of NOx and ozone as more NOx was mixed out of layer 1. TKE and MYJ performance were similar to each other; both were worse than OB70, but better than CMAQ and YSU.

CMAQ, YSU, and TKE all had much higher Kv's between 400 and 1000m, but these could not compensate for the low Kv's near the surface. If the 1 m²/s minimum had been applied over Hinton, layer 1 Kv's would have been higher in all but OB70. This patch would have benefited CMAQ, TKE, and YSU Kv's more than a KV100 or KV200 patch because none of these profiles exceeded 1 m²/s in the lowest 200 m.

Table 3-6. Comparison of 7 PM layer 1 vertical diffusivities, ozone and NOx at Hinton when using WRF/MYJ meteorology.

Kv Method	Kv (m ² /s)	Ozone [ppb]	NOx [ppb]
Observed	--	55	17
OB70	1.8	42	25
YSU	0.3	4	75
CMAQ	0.1	2	86
TKE	0.5	13	57
MYJ	0.8	15	53

Up to this point, vertical profiles have been shown only for the urban site at Hinton. Figure 3-15 shows that ozone titration by NOx is also a problem at less urban sites such as Eagle Mountain Lake. Although the buildup of NOx in layer 1 is not as large as over Hinton, ozone titration remains too high as Kv's in all methods besides OB70 are below 1 m²/s in the lowest 100 m and strong ozone and NOx gradients build between CAMx layers 1 and 2.

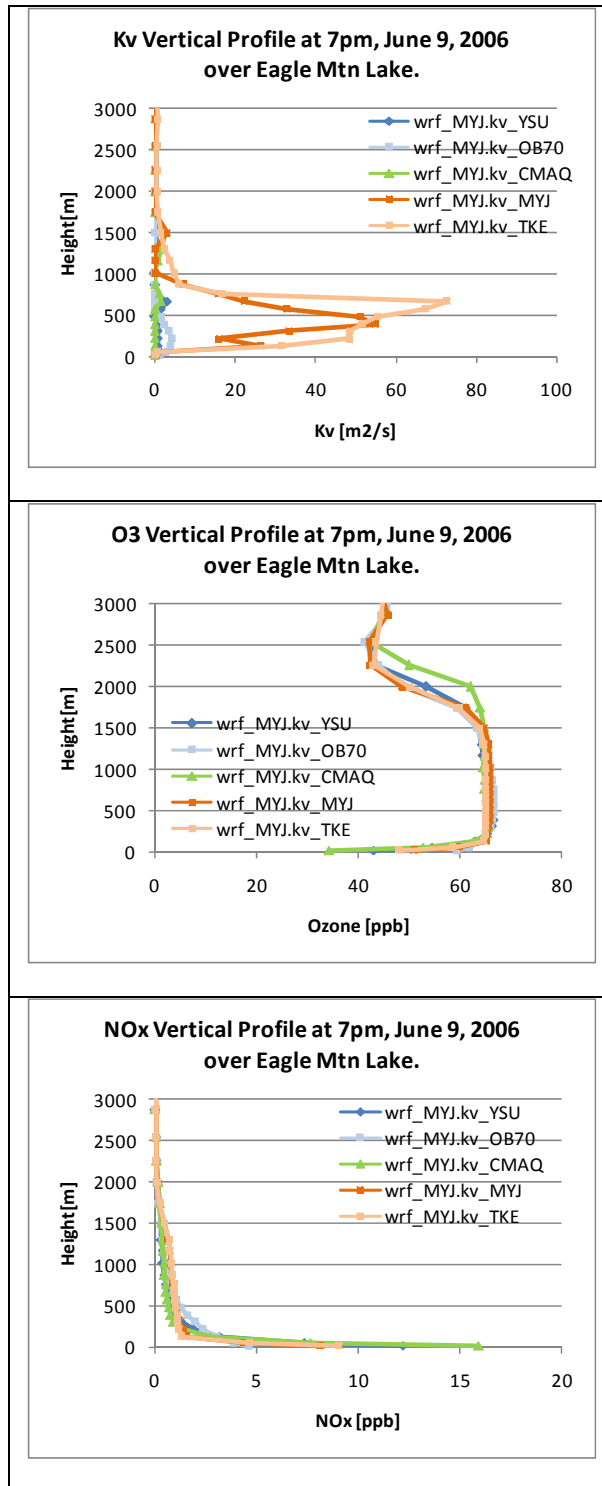


Figure 3-15. 7 PM vertical profiles of Kv (top), ozone (middle), and NOx (bottom) at Eagle Mountain Lake on June 9 from five CAMx runs using WRF/MYJ meteorology.

4.0 Findings and Discussion

Eight CAMx sensitivity tests were performed for the June 7 – 10 period of the DFW 2006 ozone modeling period to evaluate the performance of two new vertical diffusivity methods implemented into the WRFCAMx converter – YSU and MYJ. Three different diffusivity fields were generated from the WRF outputs that were configured with the YSU PBL scheme (OB70, CMAQ, and the newly implemented YSU option). Five sets of diffusivity fields were evaluated based on WRF outputs using the MYJ PBL scheme (OB70, CMAQ, YSU, the existing TKE method, and the new MYJ option). No Kv patches were applied in any of the runs.

Results from both sets of WRF meteorology show that OB70 had the lowest daytime diffusivities in almost all layers within the PBL, which led to the highest concentration of both surface layer NO_x and ozone. At night, near-surface OB70 Kv's were usually higher than the other methods, helping to mix out some of the excessive NO_x that the other methods confined to the surface layer, and helping reduce the titration of ozone. Because OB70 showed the best performance at night for both ozone and NO_x, and can perform well in the daytime too, especially when the other meteorological variables lead to an under prediction in ozone, it should remain an option in WRFCAMx. Another idea may be to use OB70 as a replacement of the arbitrary KV100 or KV200 patches that are most effective at night and early morning hours.

The YSU method, which was considered a replacement for OB70, offered more vertical mixing than OB70 in the daytime, and slightly lower daytime ozone peaks, but does not allow sufficient vertical mixing out of the surface layer at night. CMAQ diffusivities, which were consistently some of the highest in the daytime throughout the PBL, created too much vertical mixing, usually suppressing daytime ozone peaks below other Kv methods. The CMAQ Kv's could be useful if the model has a consistent positive bias in the daytime. CMAQ and YSU were often the methods to drop surface layer Kv's below 1 m²/s in the evenings. This could pose an issue when computing 8-hour ozone averages since the latter end of the 8-hour period could fall close to sunset for ozone simulations in the spring and fall. A patch would be essential in helping increase the low-level vertical mixing in the evenings and at night.

Among the two TKE methods, the MYJ option had smaller surface layer Kv's in the daytime compared to the original TKE, but at all other times their values were similar. Ozone time series and spatial plots of the daily maximum ozone did not show major differences between the two TKE methods since the only time their diffusivities showed large differences was when both already generated strong vertical mixing. The MYJ surface layer Kv's were often in the same range as YSU, but both TKE schemes tended to remain higher in the evening hours, helping to delay ozone titration somewhat, while YSU Kv's occasionally grew faster in the early morning hours, helping increase ozone production. Kv patches would be beneficial in all of these cases.

It is impossible to conclude that one diffusivity calculation method will always be superior to others, but it is clear that the previous and new approaches will continue to benefit from a patch that would increase Kv's in the lowest layers, especially in urban areas in the evenings, at night, and to a lesser extent, in the mornings. Both landuse-based minima and the KV100 patches (or KV200, as applied to the DFW 4 km base case diffusivities) would be effective in this

regard. However, in the latter case, there is no guarantee that the diffusivities in the lowest layers will be any greater than those found in layer 1. Perhaps, even higher minimum kv levels should be considered. A more consistent approach may be available by applying the OB70 technique as a replacement to the KV100/200 patch, and we recommend future work to implement this idea into the KVPATCH program.

All of the tests described in this report were conducted using the standard K-theory diffusion solver in CAMx, as opposed to the ACM2 solver. The main difference between the two is that ACM2 includes non-local convective transfer among layers within the daytime convective boundary layer, which is a more efficient mixing scheme. In most cases, the ACM2 solver would not lead to a significant difference in the results reported here, as it would only impact the mixing of ozone and precursors during convective hours of the daytime. Most Kv tests resulted in well mixed daytime boundary layers, so ACM2 mixing would only tend to mix toward even more constant profiles within the same boundary layer depth. However, ACM2 would impact the OB70 cases the most, since OB70 was weekly mixed on most days, leading to reduction of surface ozone and increases in concentrations aloft. There would be zero to negligible impact from ACM2 at night (or otherwise stable conditions) when ACM2 reverts to a K-theory scheme.

Other recommendations for future work include:

- Considering the opposite problem that can occur in rural areas at night, in which the surface layer does not sufficiently stabilize because internal minima (usually in TKE schemes) are used to set floor values for various parameters. This can lead to an inadequate reduction in nighttime ozone relative to rural observations, as documented by Kemball-Cook et al. (2010). Additional modifications to the patching program, the diffusivity diagnostics within the WRF-CAMx interface, or to WRF itself should be developed to address this issue;
- While not an issue in the episode examined here, it is very common for afternoon convection to develop sufficient cloud cover that shades the surface and causes very localized and sudden collapses of mixed layers, especially for those PBL parameterizations based on bulk parameterization (e.g., OB70, YSU) that dependent on surface stability and heat flux. An improved methodology to patch those PBL “holes”, or to apply an alternative non-bulk PBL scheme based on local stability (e.g., CMAQ or TKE) when such conditions are diagnosed, should be developed.

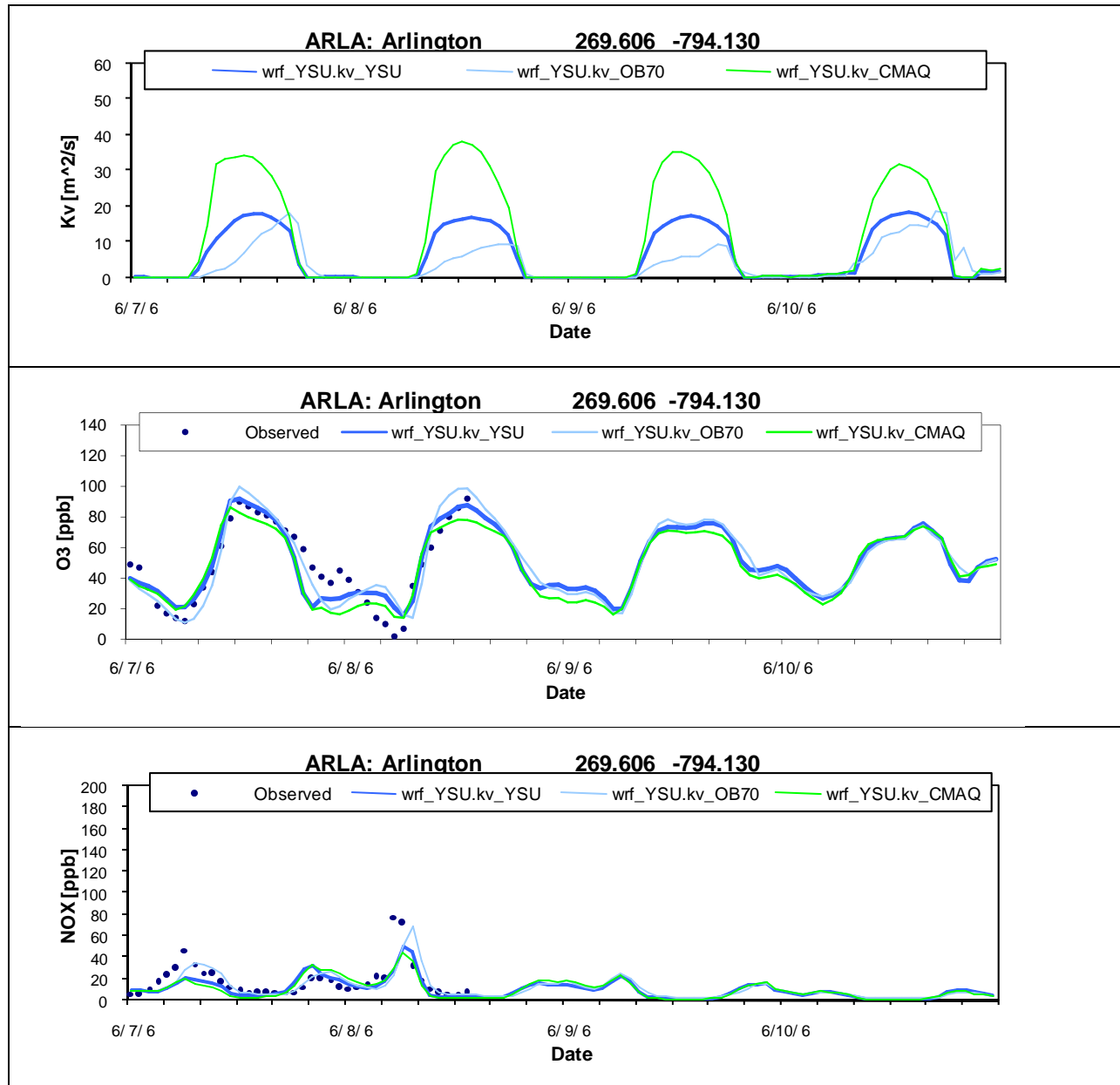
4.0 References

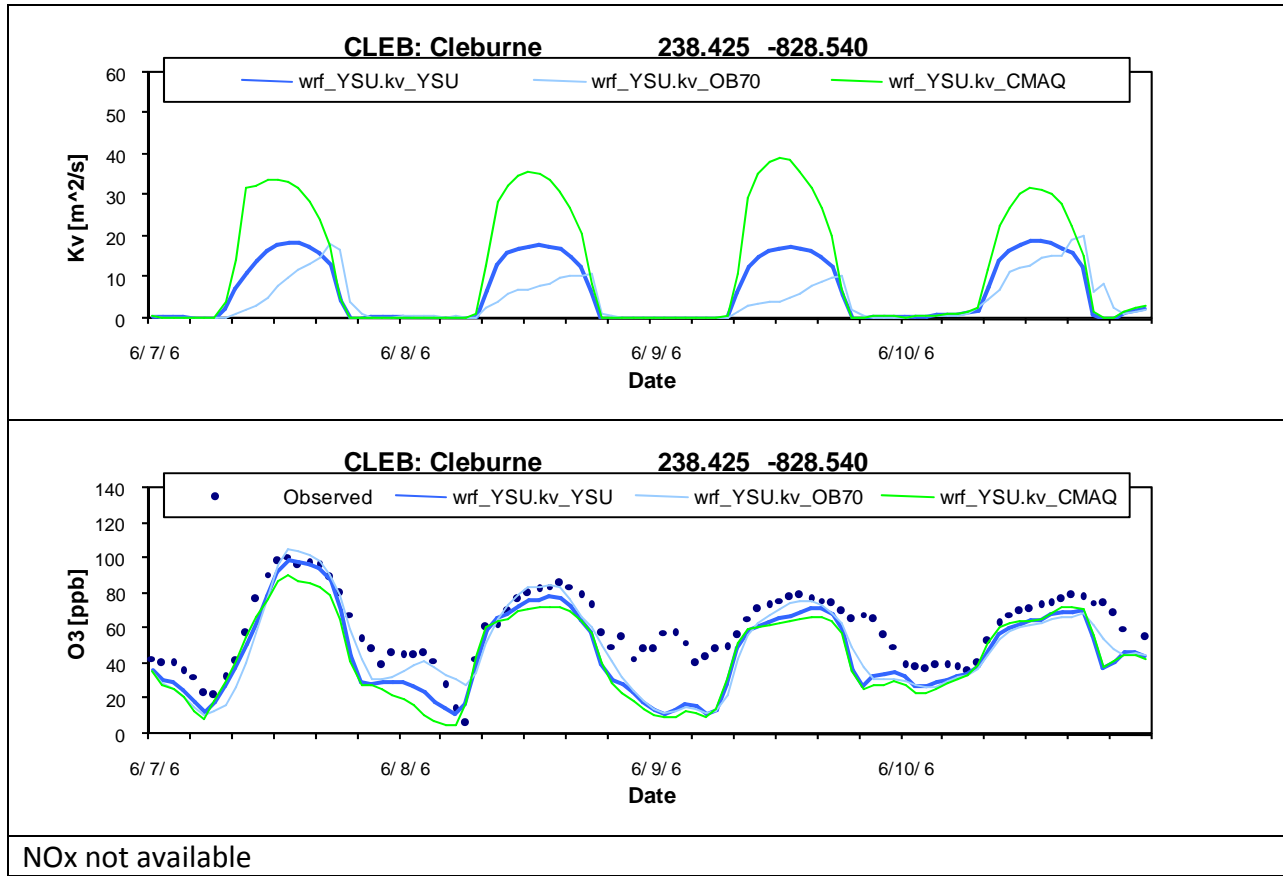
- Byun, D.W., K.L. Schere. 2006. "Review of the Governing Equations, Computational Algorithms, and Other Components of the Models-3 Community Multiscale Air Quality (CMAQ) Modeling System." *Applied Mechanics Reviews*, **59**, 51-77.
- Grell, G., J. Dudhia, and D. Stauffer. 1995. "A Description of the Fifth Generation Penn State/NCAR Mesoscale Model (MM5)." Prepared by the Mesoscale and Microscale Meteorology Division, National Center for Atmospheric Research, Boulder, CO (NCAR Technical Note NCAR/TN-398-STR).
- Helfand, H. and J. Labraga. 1988. "Design of a Nonsingular Level 2.5 Second-Order Closure Model for the Prediction of Atmospheric Turbulence." *Journal of the Atmospheric Sciences*, **45**, 113-132.
- Hong, S., Y. Noh, and J. Dudhia. 2006. "A New Vertical Diffusion Package with an Explicit Treatment of Entrainment Processes." *Monthly Weather Review*, **134**, 2318-2341.
- Hong, S. and H. Pan. 1996. "Nonlocal Boundary Layer Vertical Diffusion in a Medium-Range Forecast Model." *Monthly Weather Review*, **124**, 2322-2339.
- Janjic, Z. 1990. "The Step Mountain Coordinate: Physical Package." *Monthly Weather Review*, **118**, 1429-1443.
- Janjic, Z. 1994. "The Step-Mountain Eta Coordinate Model: Further Developments of the Convection, Viscous Sublayer, and Turbulence Closure Schemes." *Monthly Weather Review*, **122**, 927-945.
- Kemball-Cook, S., J. Jung, W. Santamaria, J. Johnson, E. Tai, M. Jimenez, G. Yarwood. 2010. "Northeast Texas Ozone Modeling of 2005 and 2012." Prepared for the East Texas Council of Governments, Kilgore TX. Prepared by ENVIRON International Corporation, Novato, CA (March 31, 2010).
- Louis, J.F. 1979. "A Parametric Model of Vertical Eddy Fluxes in the Atmosphere." *Boundary Layer Meteorology*, **17**, 187-202.
- Mellor, G. and Yamada, T. 1982. "Development of a Turbulent Closure Model for Geophysical Fluid Problems." *Reviews of Geophysics and Space Physics*, **20**, 851-875.
- O'Brien, J. 1970. "A Note on the Vertical Structure of the Eddy Exchange Coefficient in the Planetary Boundary Layer." *Journal of the Atmospheric Sciences*, **27**, 1213-1215.
- Pleim, J. 2007. "A combined local and nonlocal closure model for the atmospheric boundary layer. Part I: Model description and testing." *Journal of Applied Meteorology and Climate*, **46**, 1383-1395
- Skamarock, W.C., J.B. Klemp, J. Dudhia, D.O. Gill, D.M. Barker, M.G. Duda, X.-Y. Huang, W. Wang, J.G. Powers. 2008. "A Description of the Advanced Research WRF Version 3." Prepared by the Mesoscale and Microscale Meteorology Division, National Center for Atmospheric Research, Boulder, CO (NCAR Technical Note, NCAR/TN-475+STR, June 2008).

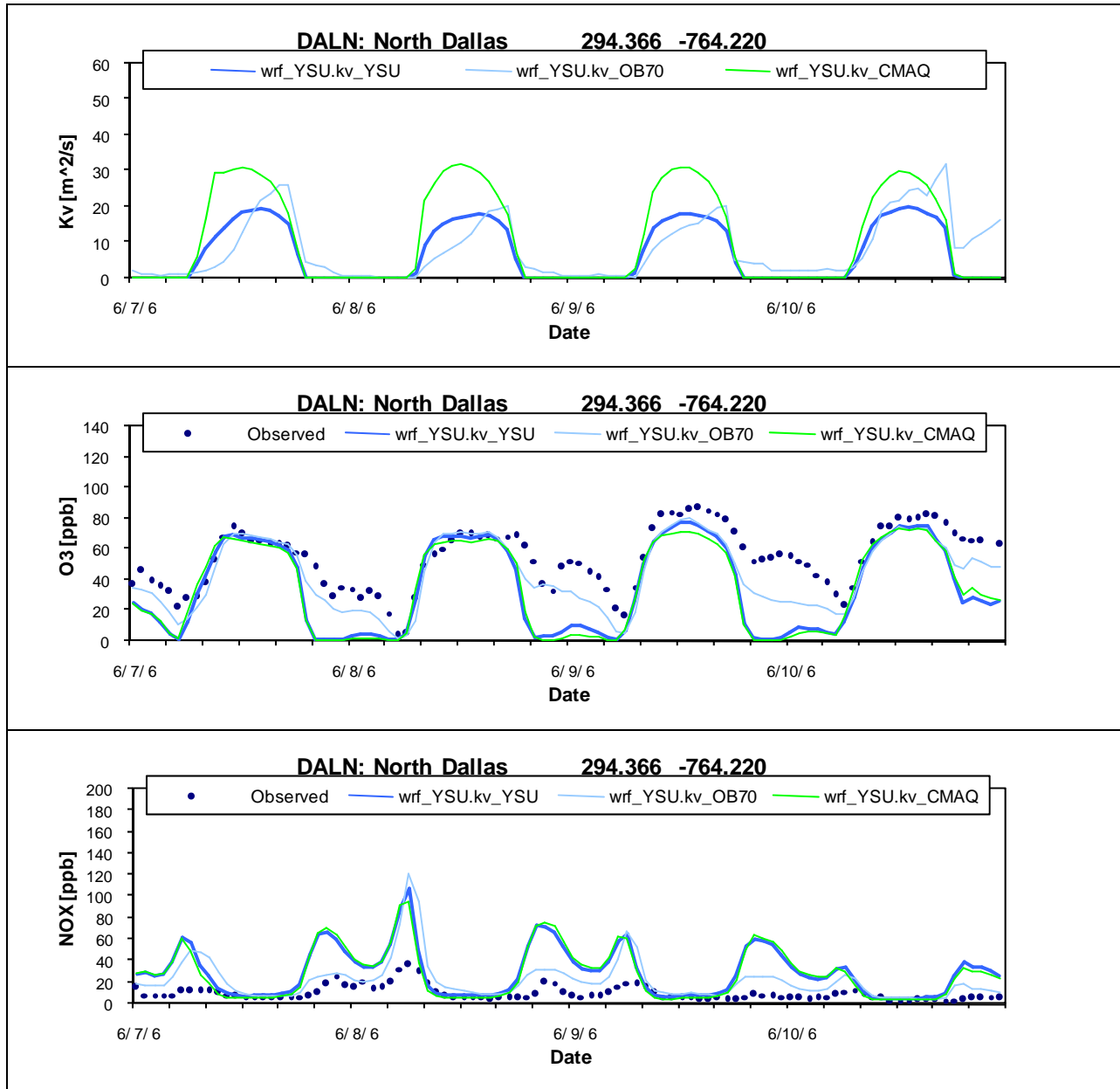
Appendix A

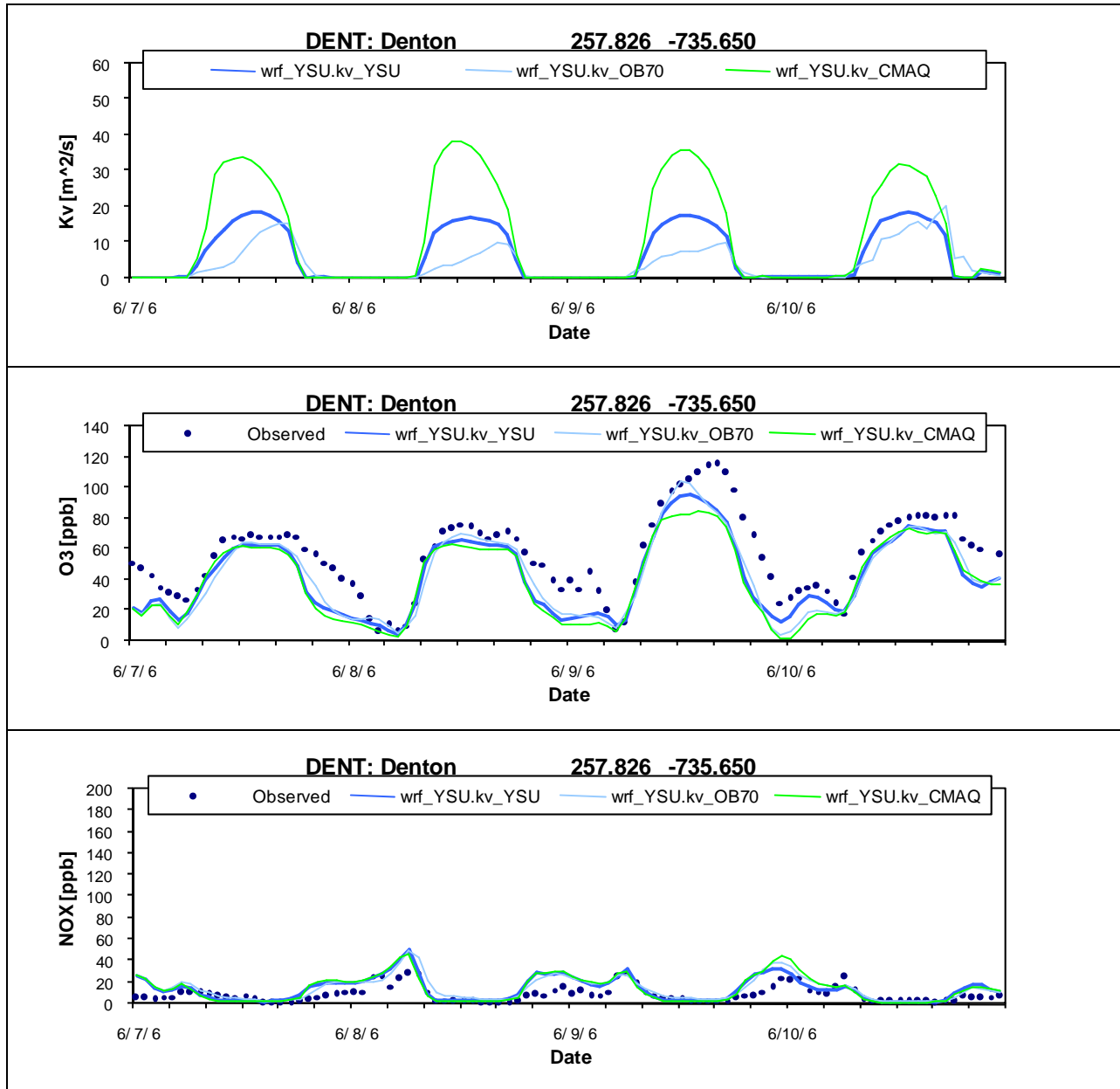
Time Series of Layer 1 vertical diffusivities, ozone, and NO_x Using Meteorology from WRF with the YSU PBL scheme

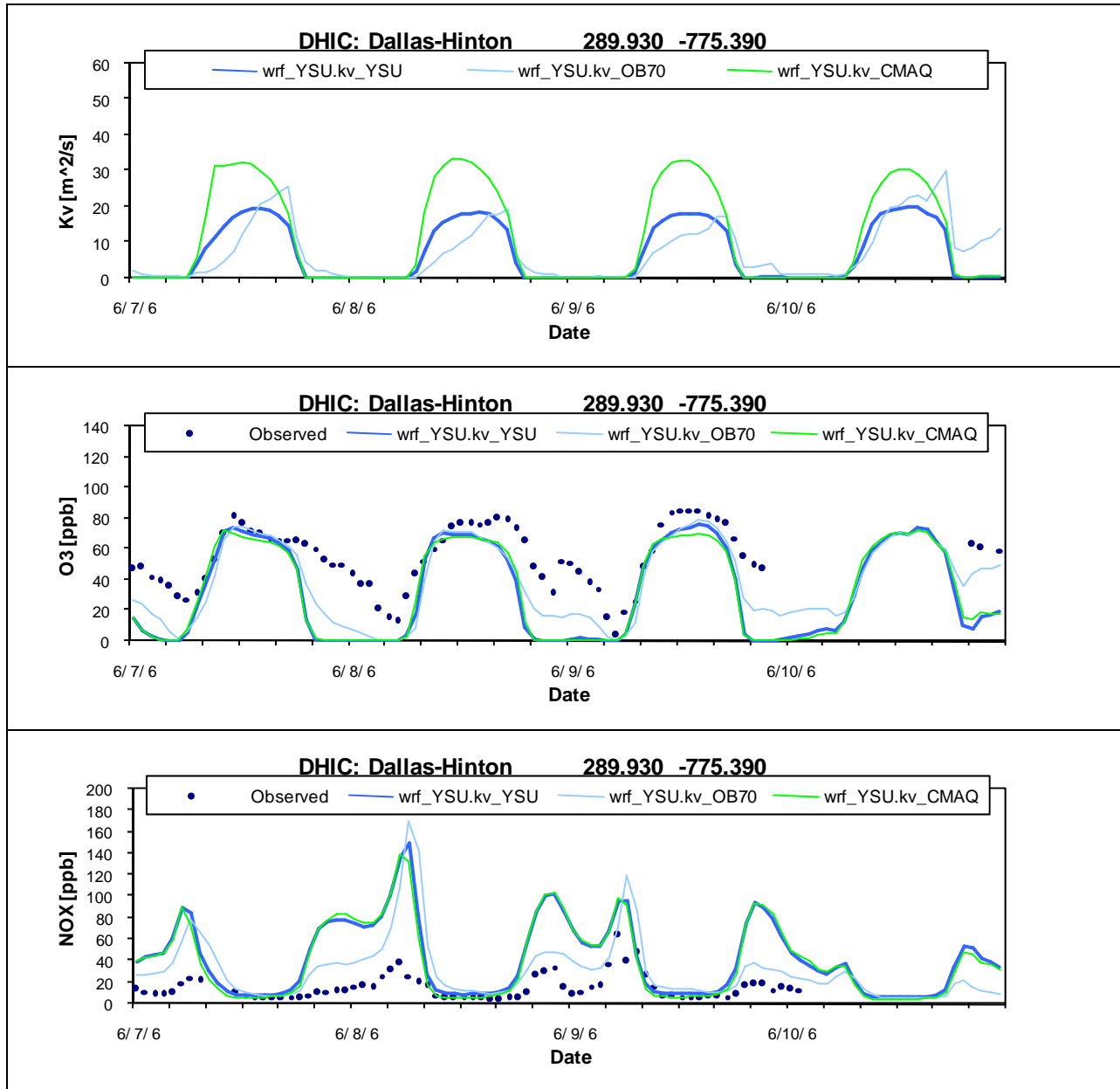
Time Series of Layer 1 vertical diffusivities, ozone, and NOx Using Meteorology from WRF with the YSU PBL scheme

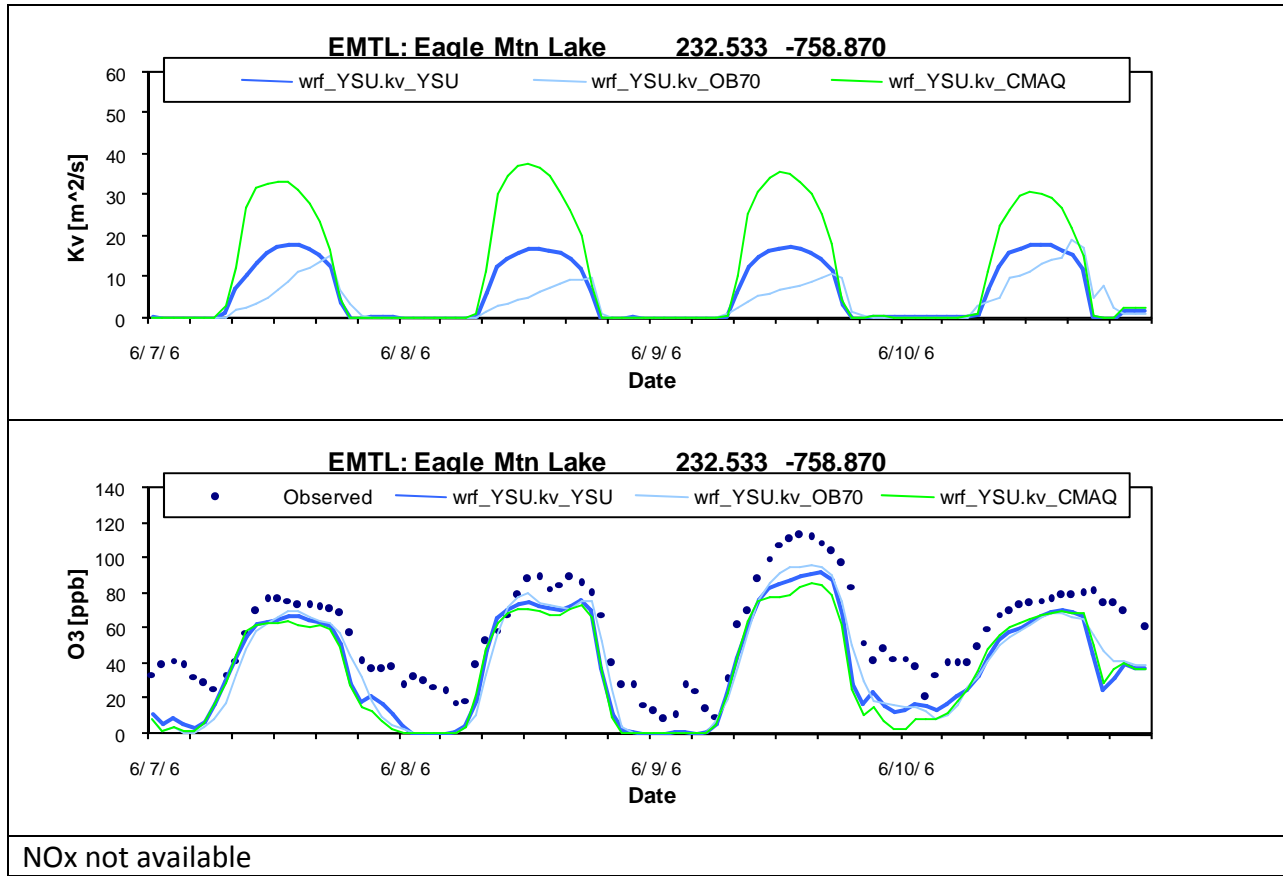


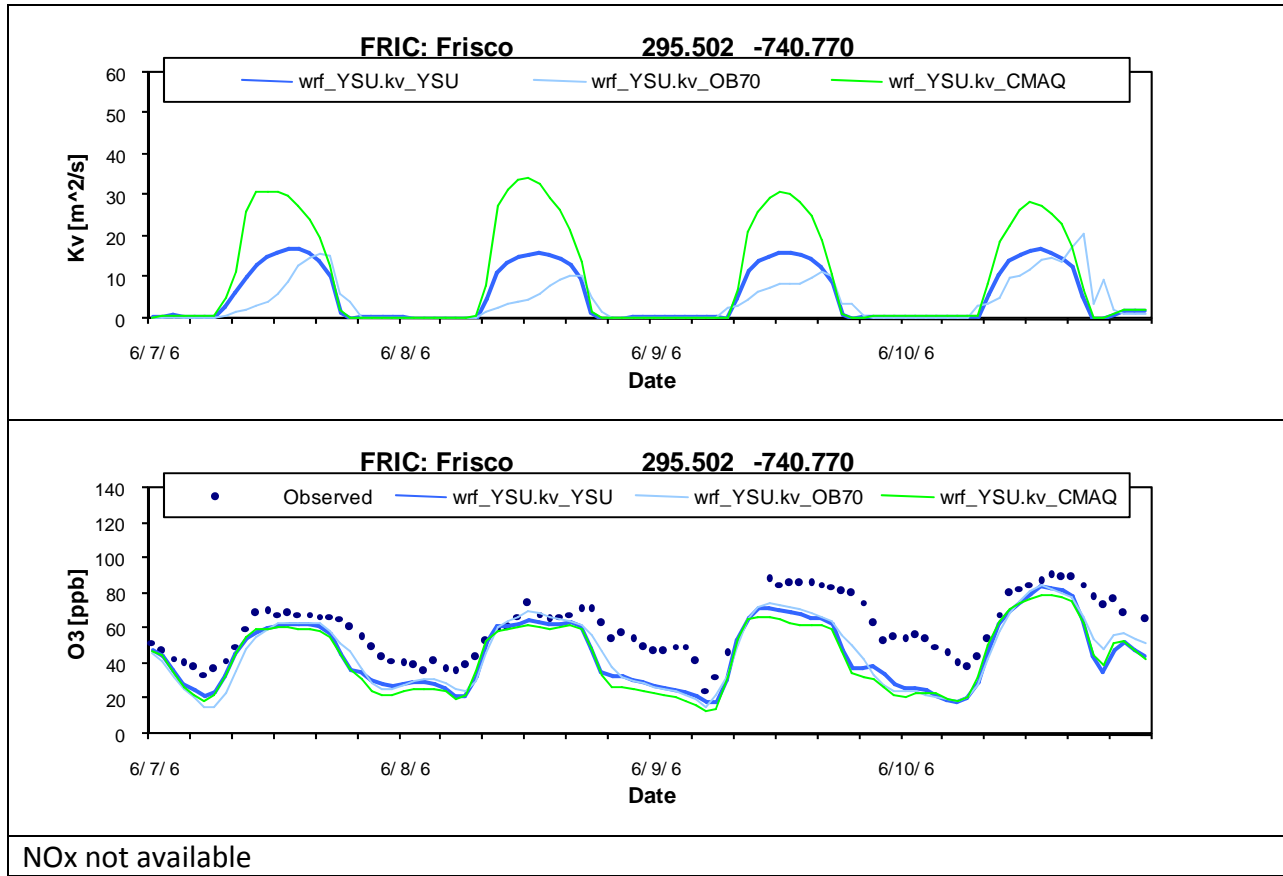


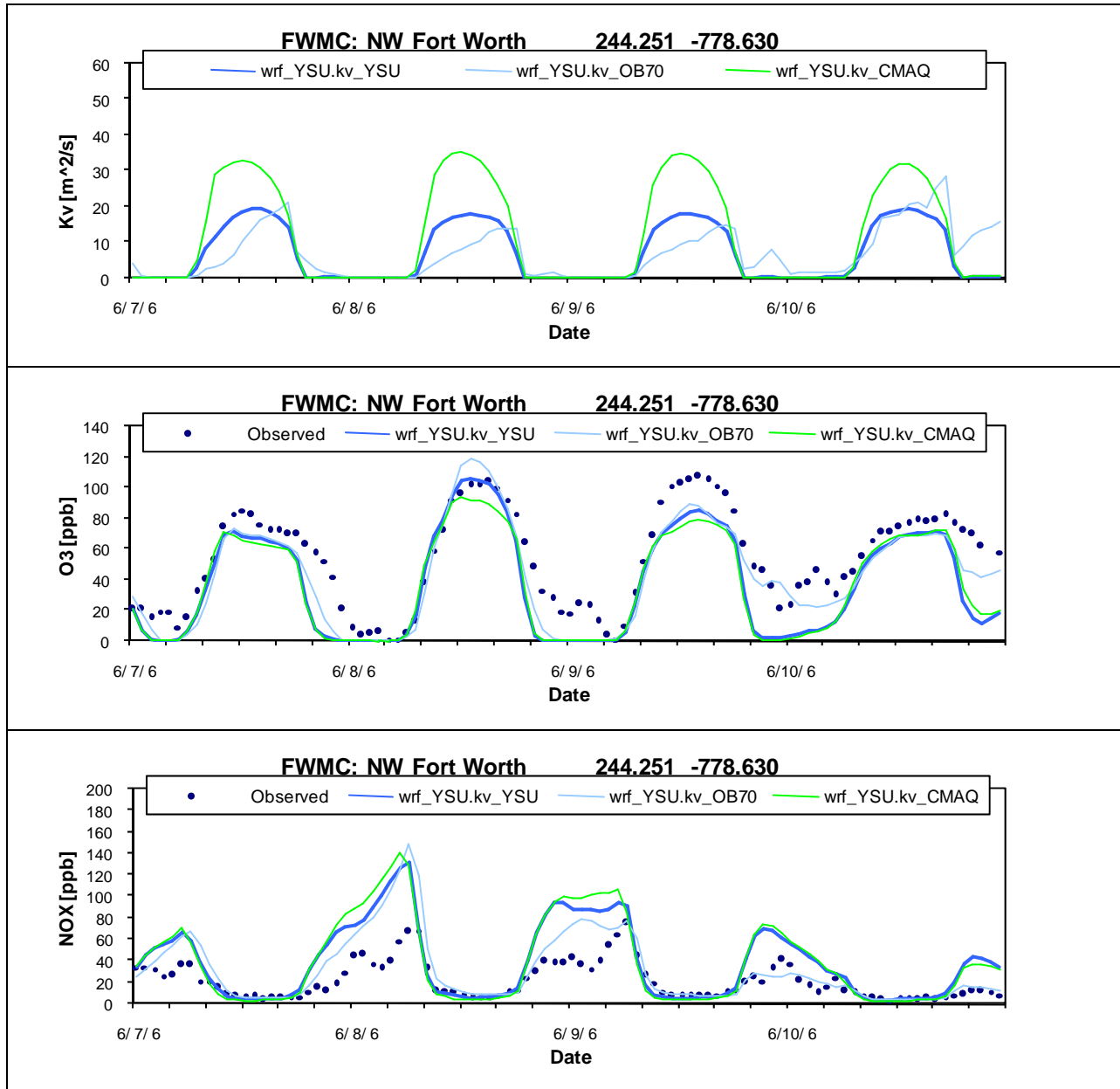


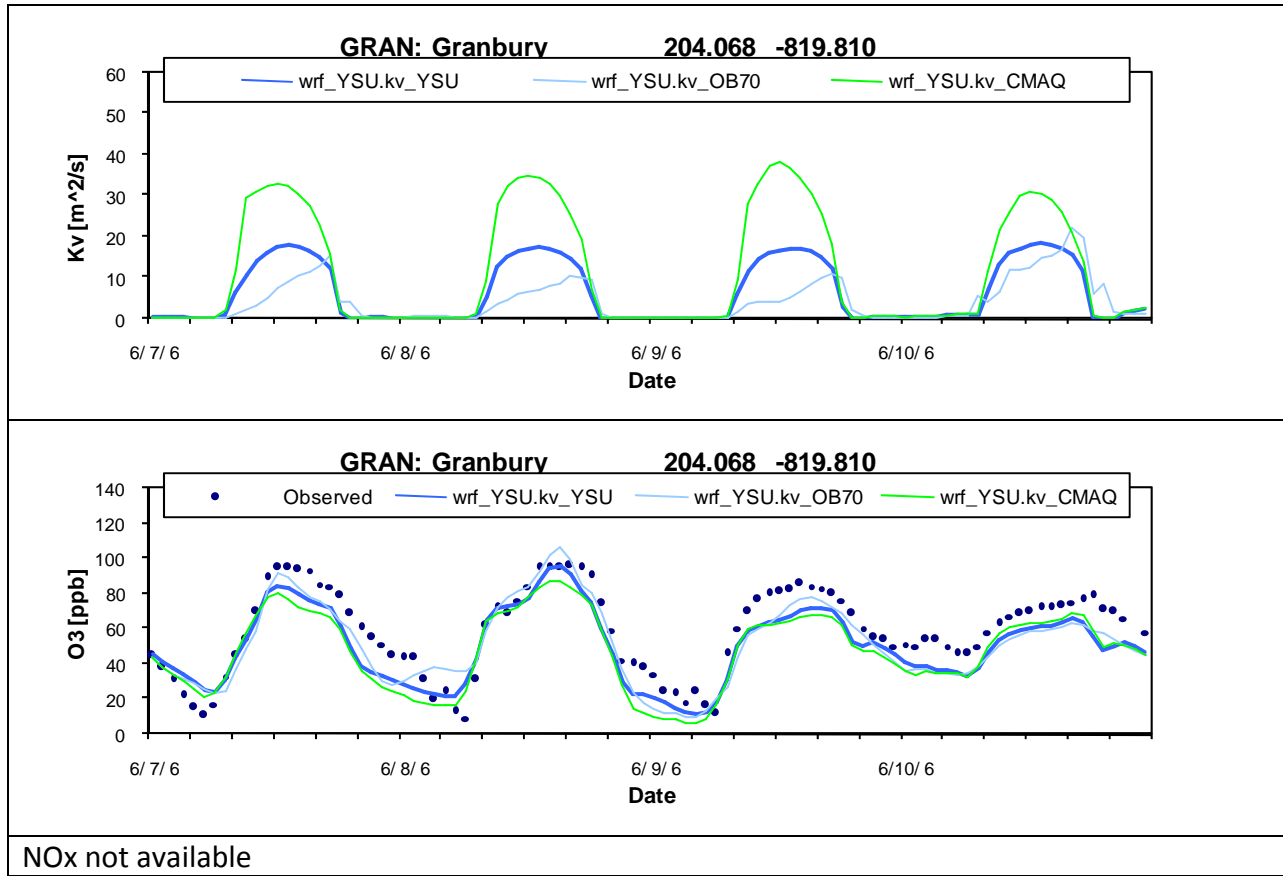


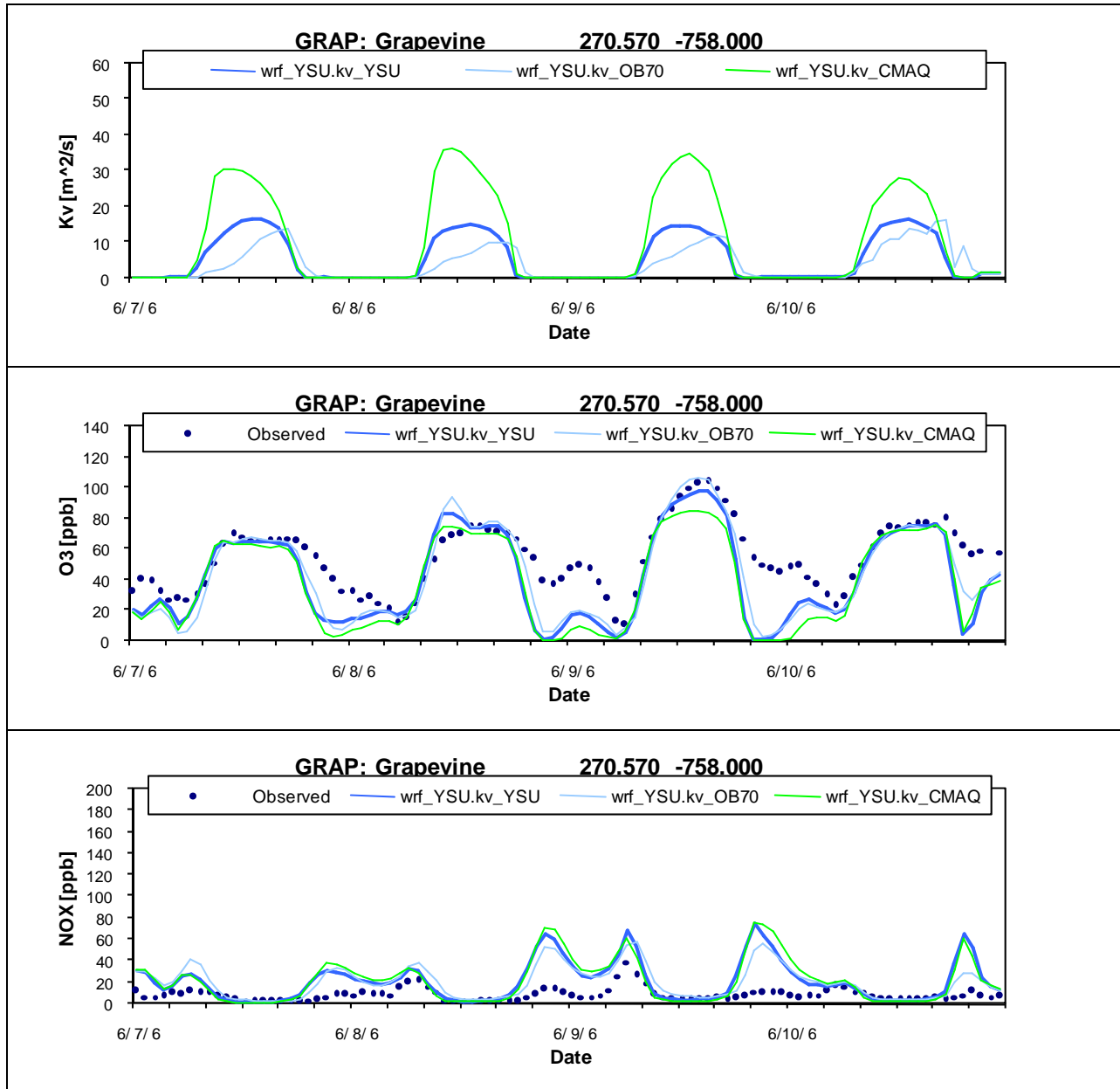


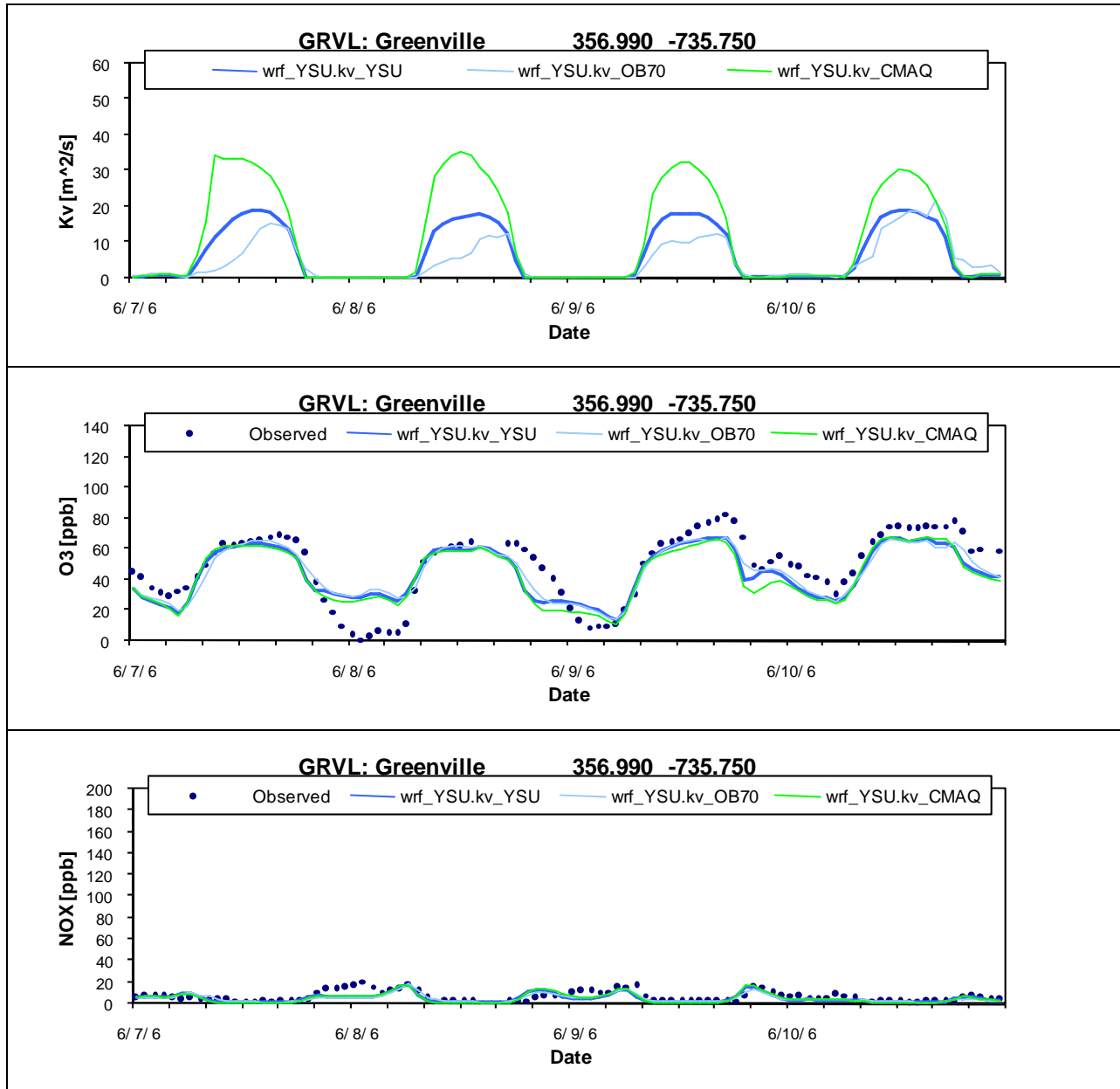


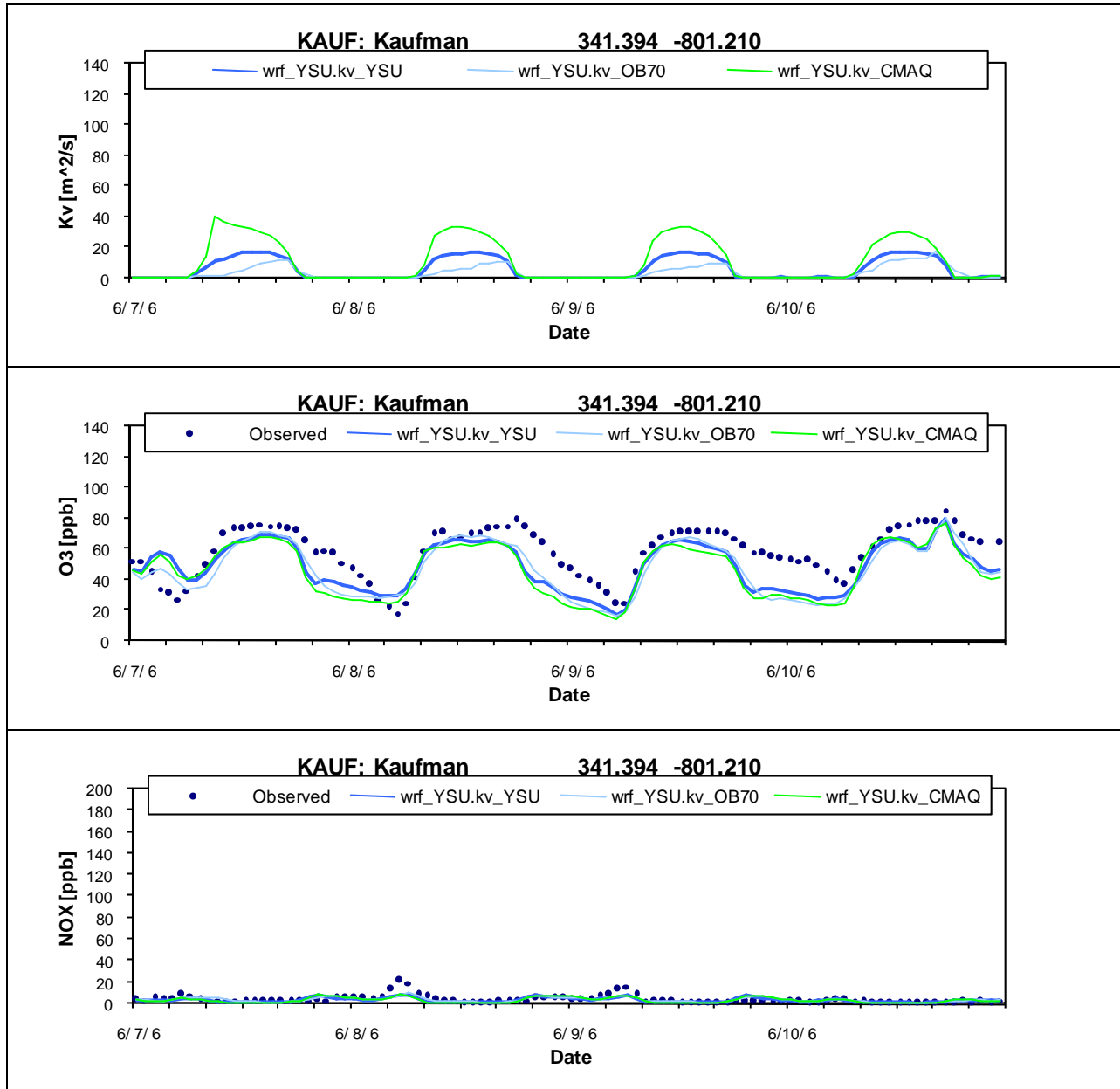


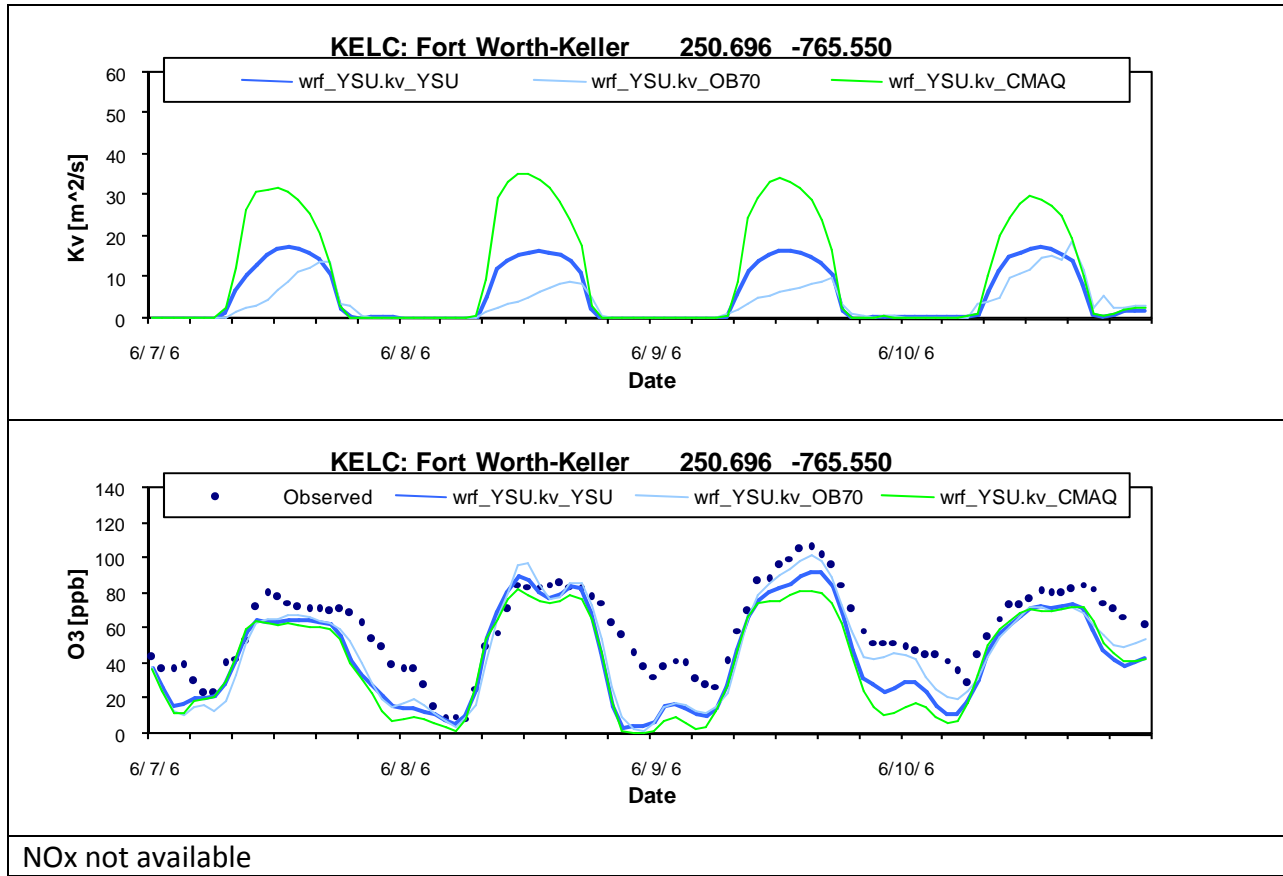


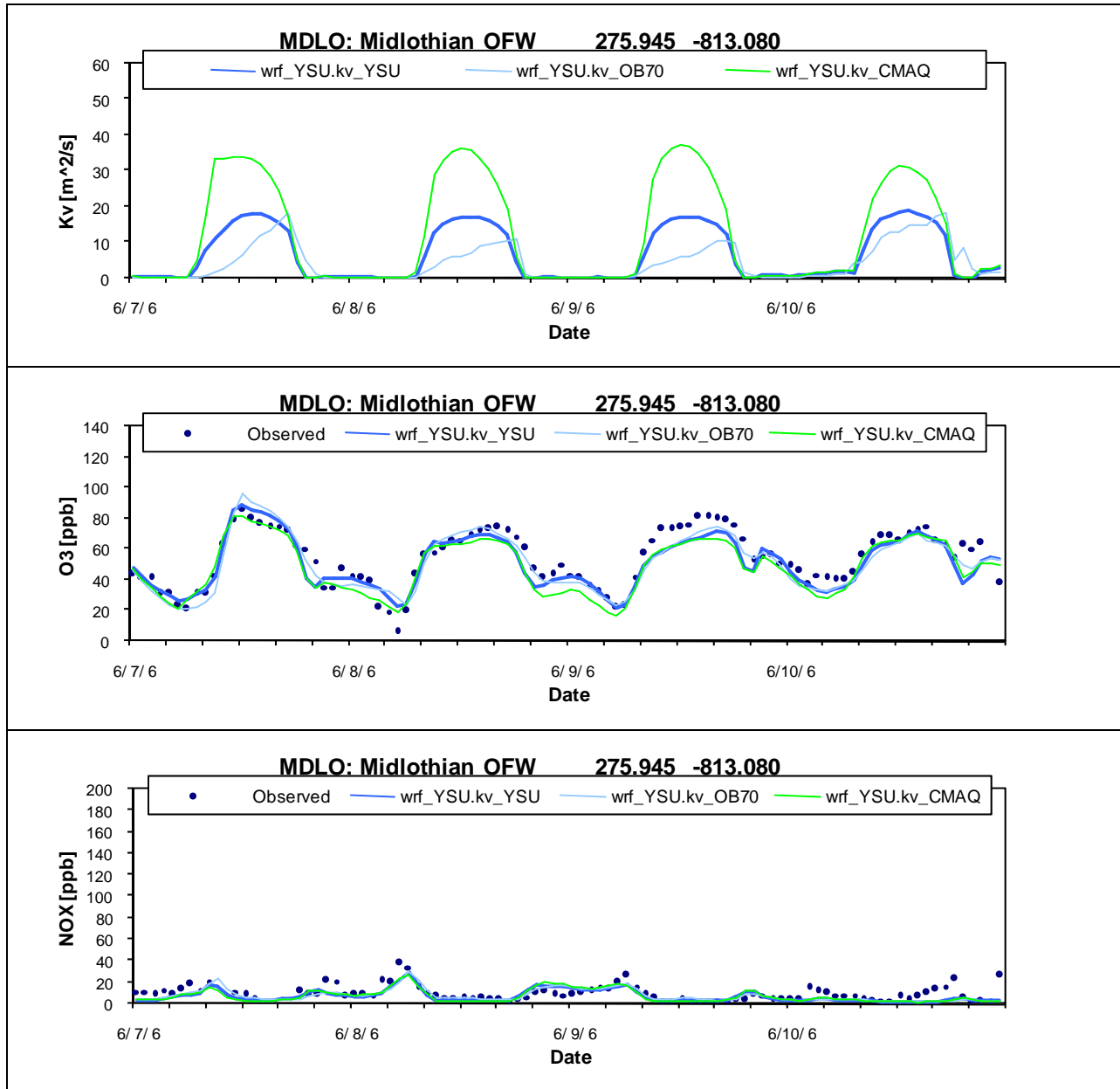


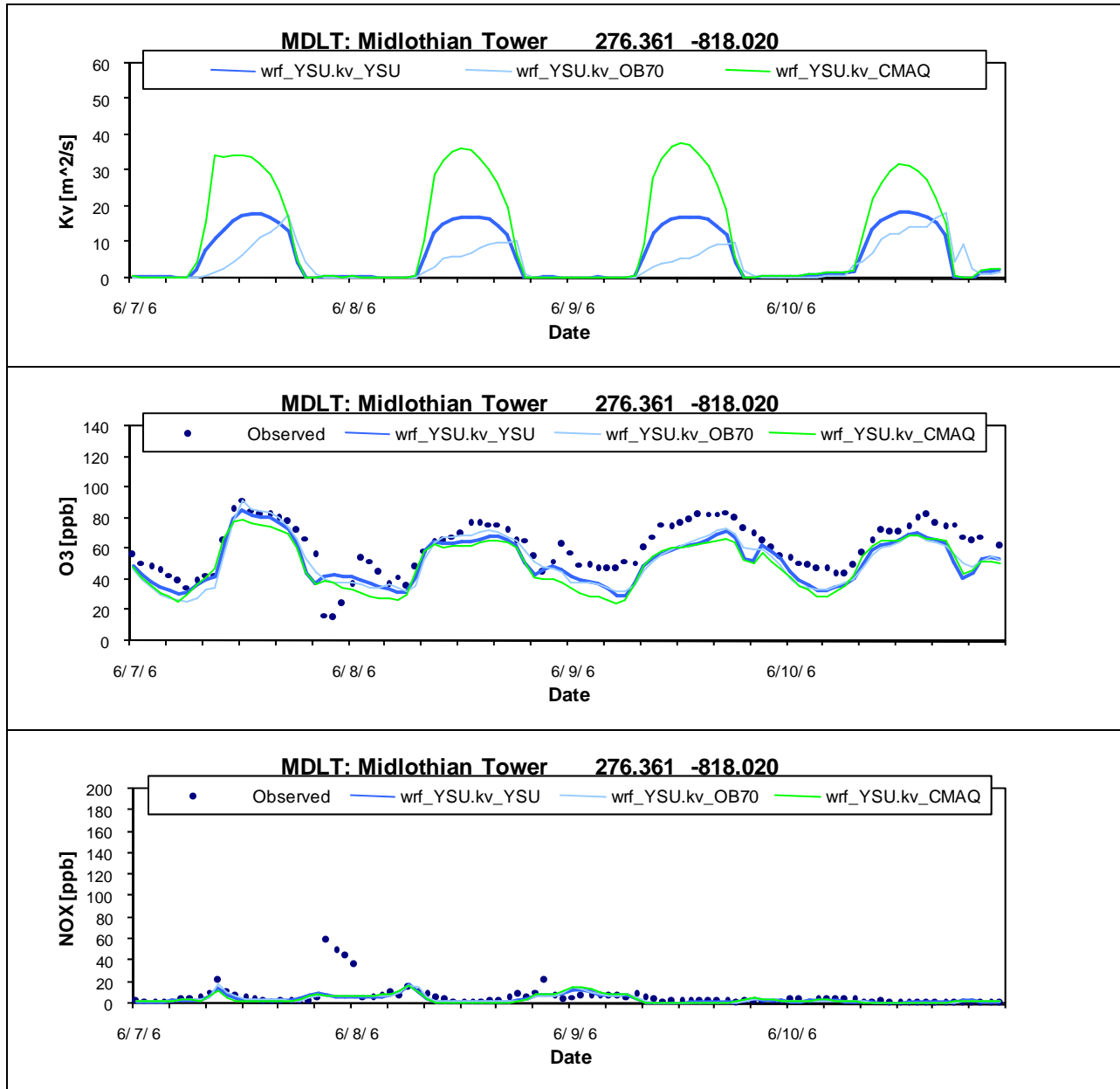


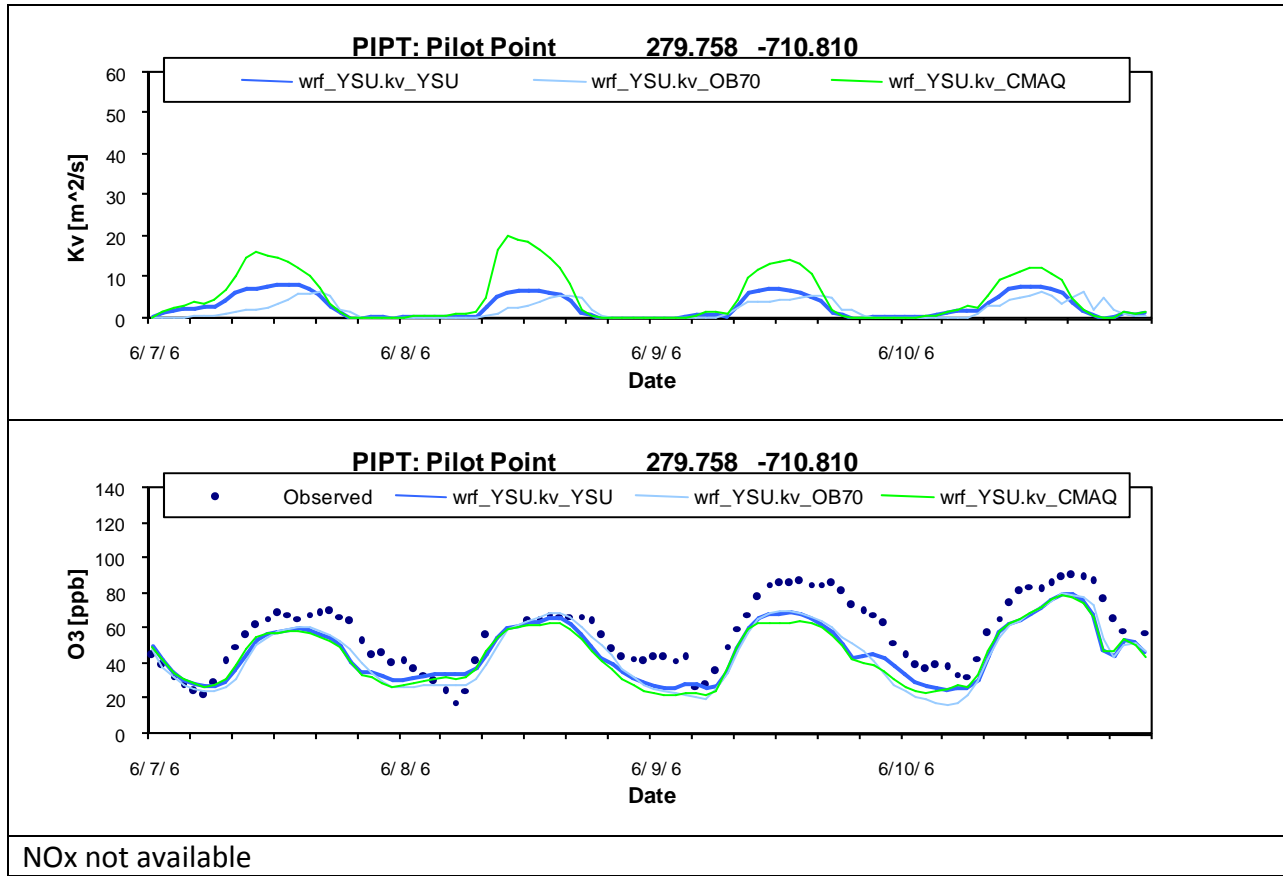


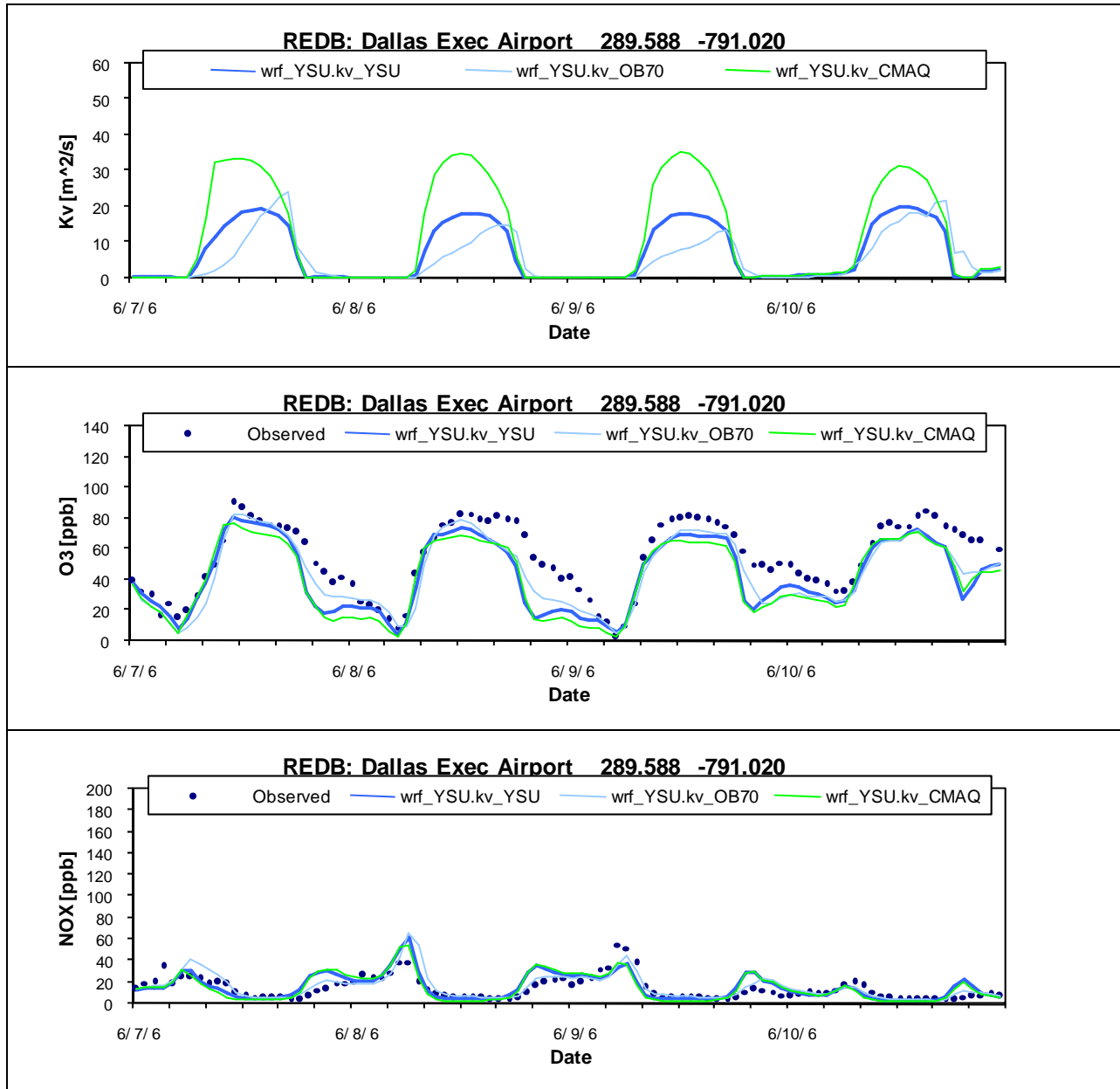


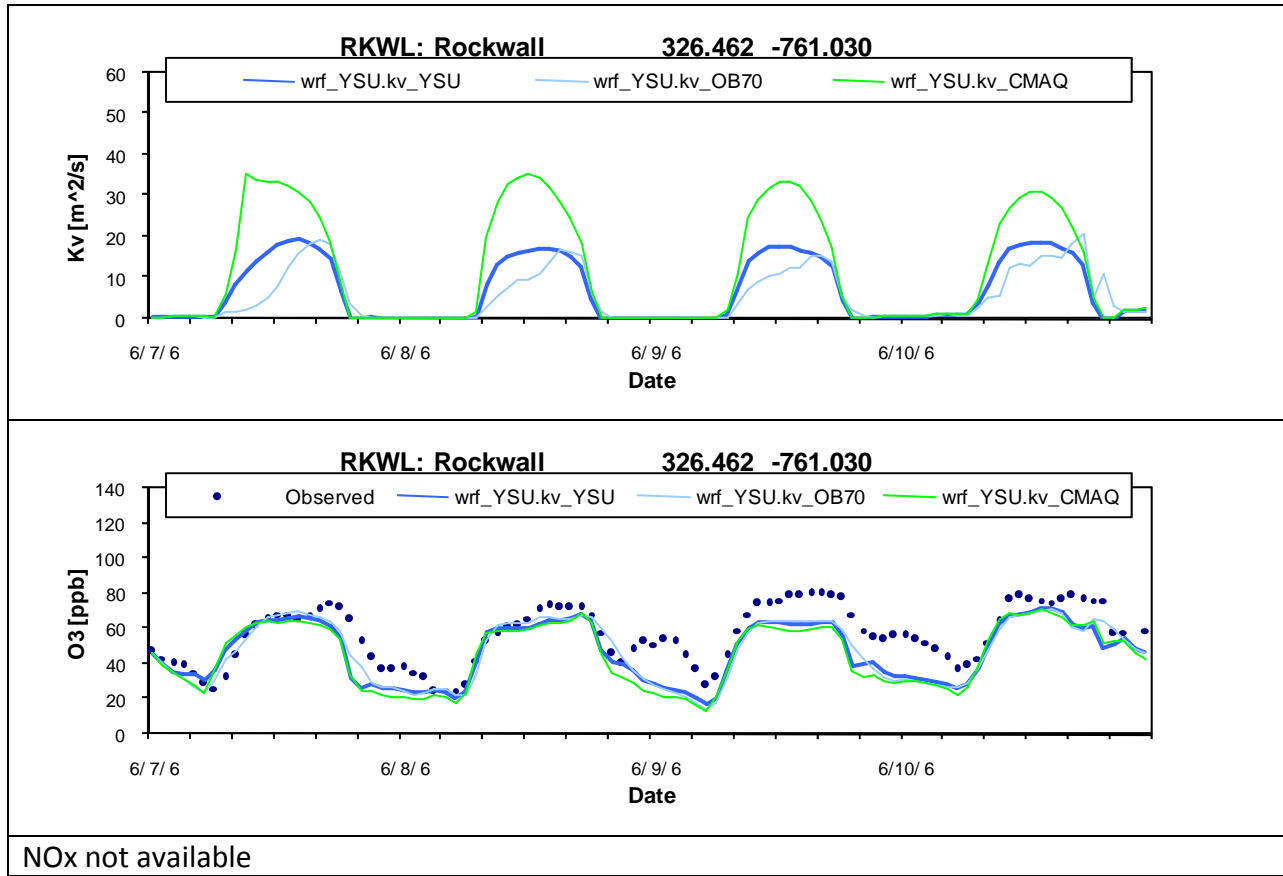


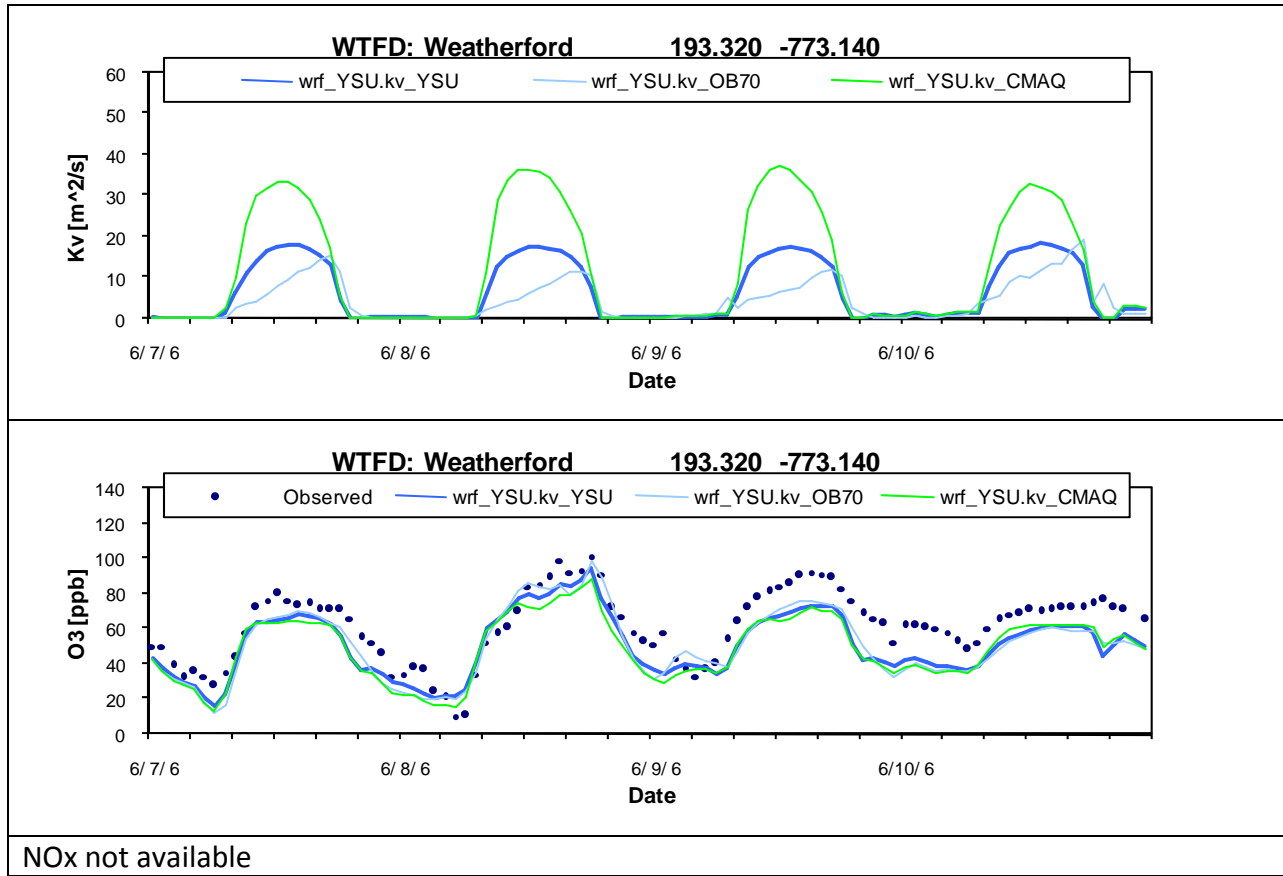












Appendix B

Time Series of Layer 1 vertical diffusivities, ozone, and NO_x Using Meteorology from WRF with the MYJ PBL scheme

Time Series of Layer 1 vertical diffusivities, ozone, and NOx Using Meteorology from WRF with the MYJ PBL scheme

